ADVANCED ENERGY MATERIALS
www.advenergymat.de

Contemporary Trends in Lithium-Sulfur Battery Design: A Comparative Review of Liquid, Quasi-Solid, and All-Solid-State Architectures and Mechanisms

*Yiheng Shao, Boyi Pang, Liam Bird, James B. Robinson, and Paul R. Shearing**

The lithium sulfur battery offers disruptive potential for applications that demand high energy density, and sustainable materials supply chains. Whilst the liquid-based Li-S technology has studied for decades, it is only comparatively recently that the chemistry has gained significant commercial traction. Historically significant and persistent challenges have hampered the technology, most pressingly, poor cyclability; however, recent efforts have demonstrated viable routes to overcome these impediments, with commercial traction increasing across the globe. These developments have addressed commercialization barriers, including the use of $LiNO_3$ as an electrolyte additive. For example, recent activity has shown progress toward more 'solid-state' conversion mechanisms, including the so-called 'quasi-solid state' system. The contemporary research landscape across liquid, quasi- and all-solid-state Li-S chemistries is reviewed. For each, a didactic overview of the underpinning operation is provided, and the literature on new mechanistic understanding, state-of-the-art characterization and materials solutions is comprehensively examined. The Li-S battery is at an inflection point in commercial deployment; this review aims to highlight the need to increase the focus of academic research on overcoming the remaining barriers to commercialization whilst continuing to identify fundamental operating mechanisms and material developments to accelerate the realization of the potential of this chemistry.

1. Introduction

The need for renewable energy storage and the urgency to decarbonize transportation greatly underscores the importance of advancing beyond current lithium-ion (Li-ion) battery technologies to meet the demands of future applications while achieving net zero goals. Among the potential solutions for next-generation battery chemistries, lithium-sulfur (Li-S) batteries hold significant promise as a successor to conventional Li-ion batteries, offering an inherently lightweight and potentially more cost-effective solution for energy storage.[1–3] This is due to its lower raw material costs, higher gravimetric energy density offered by the sulfur positive electrode, and an operational mechanism that enables functionality across a broader temperature range in comparison with conventional batteries.[4] As Li-ion batteries approach their theoretical energy density (e.g. 387 Wh kg^{-1} for $Li_{0.5}CoO_2$/ Graphite), the highly realistic energy density of Li-S batteries (likely in excess of 600 Wh kg^{-1}) significantly pushes the boundaries of possibility for next-generation batteries.[5,6]

With growing societal emphasis on safety, Li-S batteries have demonstrated clear benefits and challenges over conventional technologies. These benefits arise from the redox chemistry and conversion mechanism, which is according to the formation and conversion of lithium polysulfides (LiPS) during charge and discharge processes.[7] This eliminates the need for Li-ion intercalation into host structures, significantly reducing the risk of catastrophic battery failure by removing the metastable materials, which enable

Y. Shao, L. Bird, P. R. Shearing
The ZERO institute
University of Oxford
Holywell House
Osney Mead, Oxford OX2 0ES, UK
E-mail: paul.shearing@eng.ox.ac.uk

The ORCID identification number(s) for the author(s) of this article can be found under https://doi.org/10.1002/aenm.202503239

DOI: 10.1002/aenm.202503239

Y. Shao, L. Bird, P. R. Shearing
Department of Engineering Science
University of Oxford
Parks Road, Oxford OX1 3PJ, UK

Y. Shao, B. Pang, L. Bird, J. B. Robinson, P. R. Shearing
The Faraday Institution
Quad One
Harwell Science and Innovation Campus
Becquerel Avenue, Didcot OX11 0RA, UK

B. Pang, J. B. Robinson
Advanced Propulsion Lab (APL)
University College London
Marshgate, London E20 2AE, UK

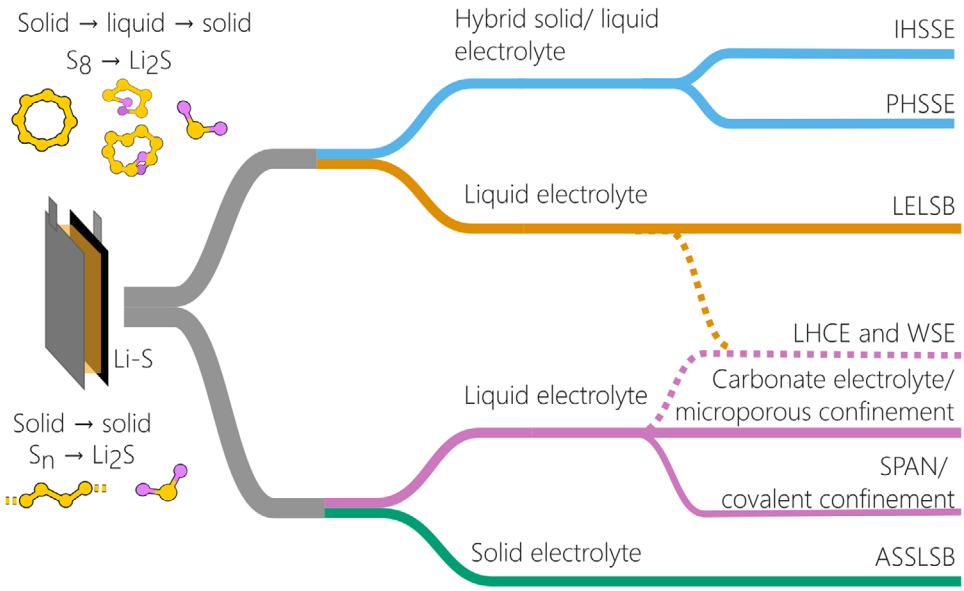

Figure 1. A 2D taxonomy of lithium-sulfur systems referred to in this review, categorized by both electrolyte type and active material conversion mechanism. LELSB: liquid electrolyte Li-S battery, LHCE: localized highly concentrated electrolyte, WSE: weakly solvating electrolyte, SPAN: sulfurized polyacrylonitrile, PQSSE: polymer-based quasi-solid-state electrolyte, IQSSE: inorganic-based quasi-solid-state electrolyte, ASSLSB: all-solid-state Li-S battery. Here, for the purposes of simplifying the taxonomy, we have classified the varying cell types according to the principal, theoretical reaction mechanism, recognizing that in practice multiple parallel reaction mechanisms may co-exist. Note that the conversion mechanism in LHCE and WSE involves both solid–solid and solid–liquid–solid pathways.

thermal runaway in Li- and Na-ion batteries. It should, however be noted that this mechanism does not preclude the possibility of thermally driven failure in Li-S cells. The conversion mechanism also allows Li-S cells to be stored safely for long periods and transported in a fully discharged state, unlike Li-ion cells, which become unstable at low states of charge.[8] The reduction reaction of $LiNO_3$ electrolyte additive contributes to the incorporation of a protective solid-electrolyte-interphase (SEI) layer at the lithium anode surface, which not only physically mitigates short-circuit risks but also enhances safety further by inhibiting the reduction reaction of LiPS.[9] However, studies have shown that $LiNO_3$ additives can also act as a threat to the operational safety of Li-S batteries. The $LiNO_3$ can be decomposed into oxidizing gases and highly reactive intermediates under high temperature, which triggers the side reactions that release a huge amount of heat.[10] The heat accumulated inside the cell can accelerate the further decomposition of $LiNO_3$ and its side reactions, which can eventually lead to exothermic thermal failure.[11] Additionally, the use of $LiNO_3$ as an electrolyte additive is incompatible with the UN Recommendations on the Transport of Dangerous Goods,[12] due to gas evolution from $LiNO_3$ and therefore cell volume expansion.[10] However, the safety concerns associated with $LiNO_3$ have received little attention so far. Therefore, a comprehensive summary of both advantages and the limiting factors related to $LiNO_3$ for Li-S batteries is of critical importance.

Solid-state batteries and quasi-solid-state batteries have been introduced and studied to tackle the polysulfide "shuttle effect" which acts as a significant obstacle in Li-S battery commercialization. In these two emerging electrolyte-system configurations, the mitigation of the shuttle effect suppresses the reaction between lithium metal and LiPS, leading to enhanced lithium anode stability and thereby prolonging battery lifespan[13] and removing the need to include $LiNO_3$ as an electrolyte additive, by extension, overcoming the safety concerns previously discussed. This review focuses on the energy storage mechanisms used by Li-S batteries across different electrolyte systems (namely, conventional liquid, quasi-solid state, and all-solid state), aiming to provide a comprehensive understanding of current challenges and future directions of this rapidly evolving field of research. In doing this, we aim to highlight activities that have demonstrated practically feasible cell performance without $LiNO_3$, with a view to supporting an acceleration in the technology toward commercialization and passing the established safety criteria for secondary energy storage devices.

First, we introduce and discuss the operational mechanism of $LiNO_3$ additive in conventional liquid-electrolyte-based Li-S systems (referred to as LELSB), highlighting its major limitations and practical bottlenecks. Next, alternative configurations and mechanisms of Li-S cells are systematically summarized. Liquid electrolyte systems where the active material undergoes conversion in the quasi-solid state are referred to here as a liquid electrolyte with quasi-solid-state mechanism (LEQSSM). Cells in which the active material undergoes conversion in the quasi-solid state, using a hybrid quasi-solid-state electrolyte comprising either a solvent and gel-like polymers, or a solvent with solid inorganic components, are referred to as PQSSE and IQSSE, respectively. Cells using a solid electrolyte where the active material undergoes conversion in the solid state are referred to as all-solid-state Li-S batteries (ASSLSB) (See **Figure 1**). For each system, the discussion emphasizes their advantages in addressing issues associated with $LiNO_3$. Several emerging strategies that have not yet been widely adopted but show translational potential are also

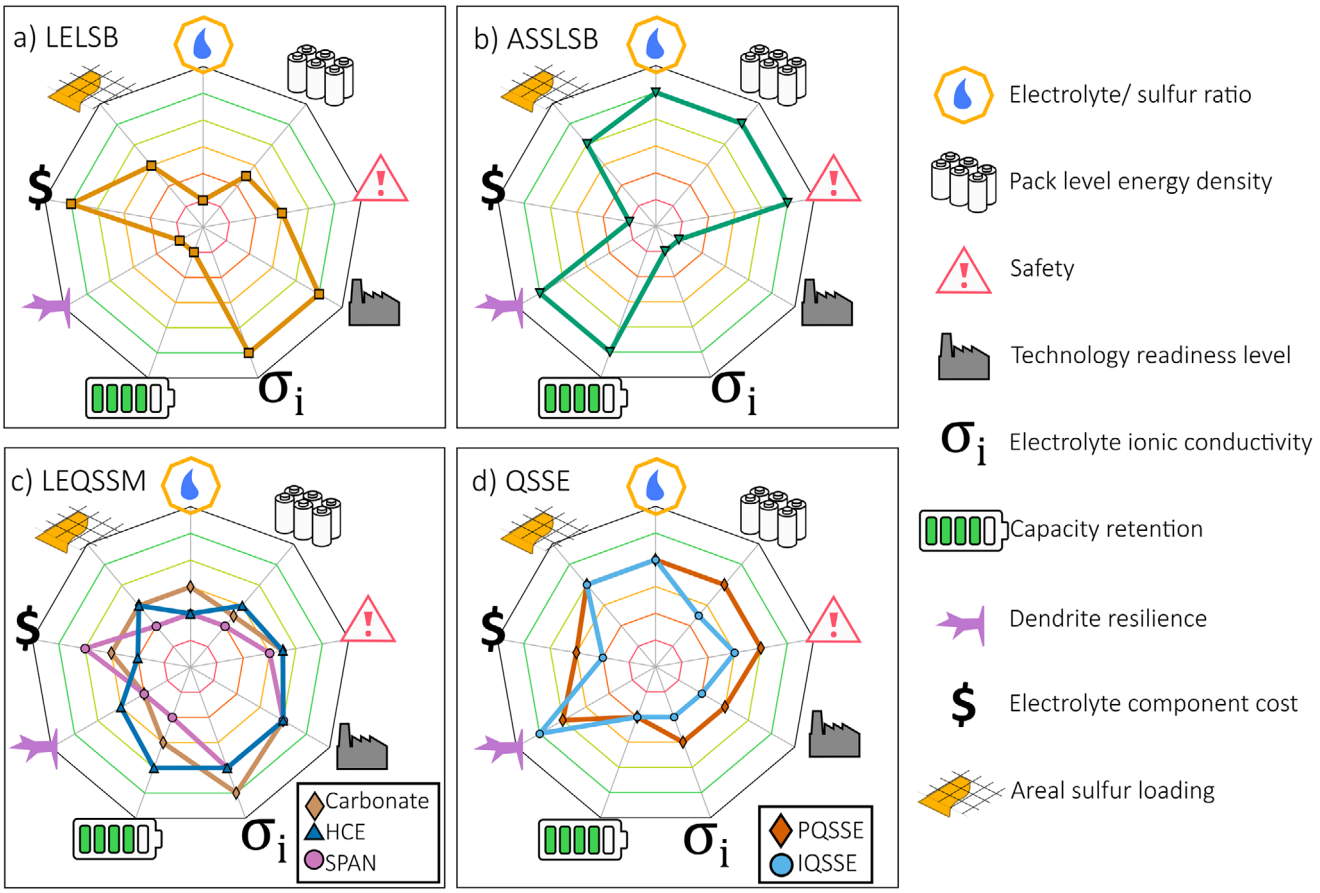

Figure 2. Radar plots summarizing key advantage and disadvantages of each Li-S electrolyte system. Radial values are assigned qualitatively based on the relative ranking of each system, with best performance at the outermost edge and weaker performance at the center. a) Liquid electrolyte Li-S batteries (LELSB), b) all solid-state Li-S batteries (ASSLSB), c) Liquid electrolyte with quasi-solid state conversion mechanism (LEQSSM) including cells with carbonate electrolyte, localized highly concentrated electrolyte (LHCE) or weakly solvating electrolyte (WSE), and sulfurized polyacrylonitrile (SPAN)-based cathodes, and d) hybrid solid state electrolyte (QSSE) cells with polymer (PQSSE) and inorganic (IQSSE) electrolytes.

discussed. Finally, conclusions and perspectives are proposed on the integrated development of $LiNO_3$-based liquid electrolyte, quasi-solid-state, and solid-state Li-S battery systems.

2. Liquid-Electrolyte Lithium–Sulfur Batteries with Liquid Mechanism

2.1. Introduction

Liquid-electrolyte-based Li–S batteries (LELSBs) are the most widely explored configuration due to their favorable intrinsic properties and compatibility with established Li-ion battery technologies. Compared to solid-state systems, liquid electrolytes offer high ionic conductivity and excellent interfacial contact with electrodes, while also facilitating the dynamic conversion reactions of sulfur species by improved electron transfer (**Figure 2**). These features collectively contribute to improved capacity utilization and enhanced energy density compared to their Li-ion counterparts.

LELSBs employ a liquid organic electrolyte contained in the pores of the separator, serving as the medium for Li-ion transport.[14] The conventional configuration of electrolyte in LELSBs includes lithium salt, solvent and additives, where each component serves specific roles. The lithium salt acts as an essential component in the Li-S battery electrolyte as a source of free Li ions for ionic conduction, which can largely determine the electrolyte properties, where lithium bis(fluorosulfonyl)imide (LiFSI) and lithium bis(fluoromethanesulfonyl)imide LiTFSI are widely used because of their robust thermal stability and high ionic conductivity.[15,16] However, compared with LiTFSI, investigations have revealed that FSI^- in LIFSI may react irreversibly with polysulfides through nucleophilic attack, leading to the formation of unstable byproducts, which not only cause the inventory loss of lithium and active materials but also compromise electrochemical stability in LELSBs.[15] In LELSBs, the electrolyte salts are dissolved in liquid solvents, with 86% of samples in a recent meta-analysis[16] using a mixture of 1,3-dioxolane (DOL) and 1,2-dimethoxyethane (DME) in a 1:1 ratio by volume (herein referred to as DOL:DME). Ether-based DME contributes to dissolving lithium salts and LiPSs and provides a medium for Li-ion transport, influencing electrolyte viscosity and thus stability, while DOL contributes to stabilizing the lithium metal against dissolved LiPSs (**Figure 3**). In particular, the low viscosity of the DOL:DME electrolyte is crucial for good rate capability at low

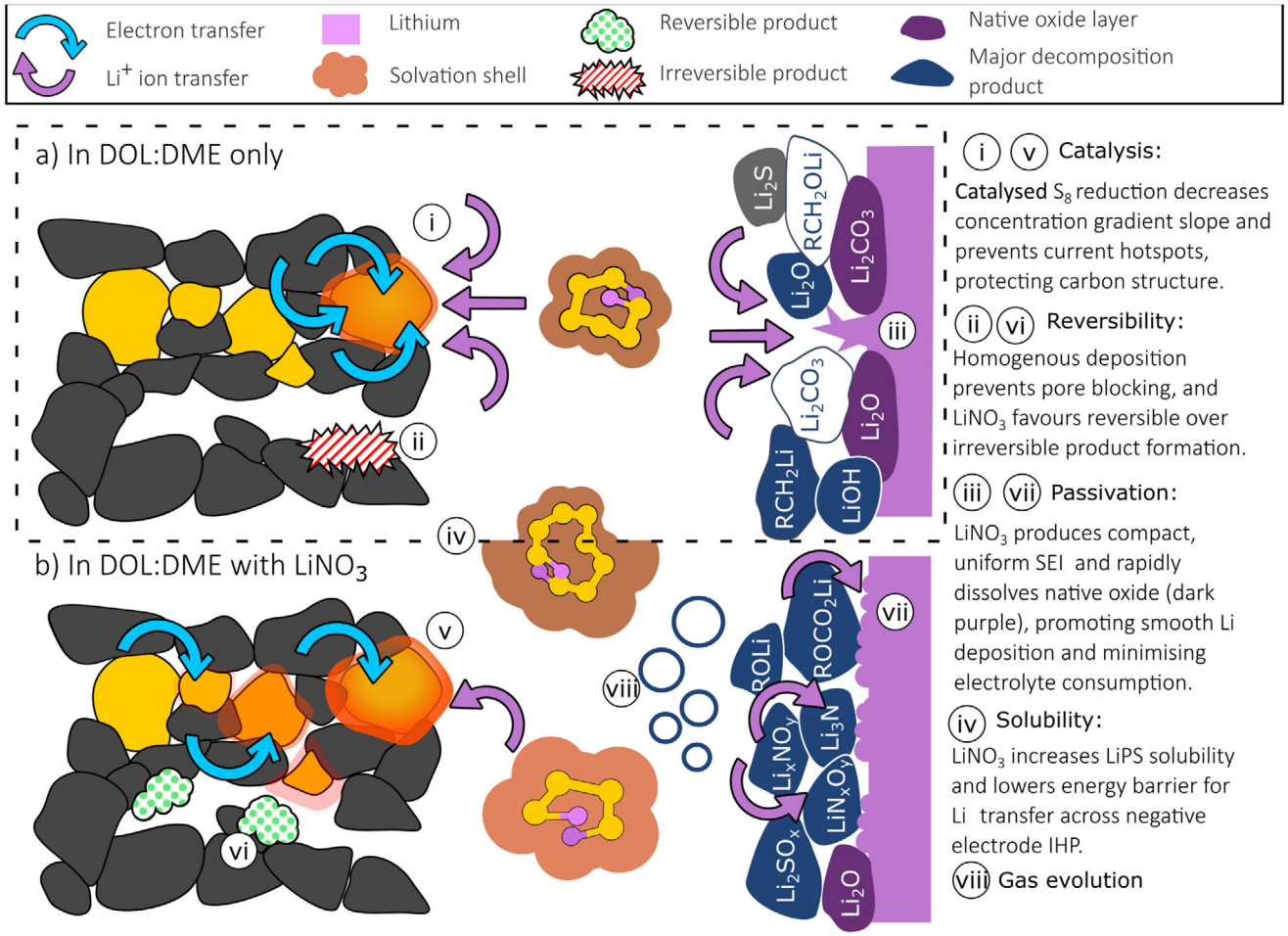

Figure 3. Effects of using DOL/DME liquid electrolyte without (a) and with (b) $LiNO_3$ additive on the positive and negative electrode interfaces. References for mechanisms illustrated: catalysis and reversibility;[2,11] SEI species[2,29,30] solubility;[29] gas evolution.[10,31]

temperatures and readily dissolves elemental sulfur, which enables the redox reactions of sulfur to occur in the solution.[17]

The main functions of electrolyte additives are to assist in the construction of a robust SEI layer to protect lithium anode, and to conjugate with lithium salts and solvents to minimize the LiPS dissolution and shuttle to increase the cycle stability and Columbic efficiency.

The intrinsically high solubility and mobility of intermediate polysulfides in LELSBs promote spatially heterogeneous dissolution and subsequent non-uniform deposition on both negative electrode and positive electrode during cycling (Figure 3), particularly under high current densities or lean-electrolyte conditions. This behavior severely limits the utilization of active lithium and sulfur species, degrades cyclability, and ultimately compromises the practical viability of LELSBs. In contrast, solid-state electrolyte configurations benefit from spatially confined reaction pathways, leading to potentially more uniform Li_2S deposition, despite persistent limitations in ionic transport across the negative electrode interface and mechanical mismatch arising from interfacial rigidity. The relatively high electrolyte to sulfur ratio (E/S ratio) is also an issue for the liquid system and electrolyte loading currently dominates the overall cell mass, with a significant penalty on gravimetric energy density (Figure 2a): an E/S ratio of 3–5 µL mg^{-1}_S has been widely discussed as a figure of merit required for energy density that is competitive with commercial Li-ion cells,[18–20] however this value is highly dependent upon the sulfur loading in the positive electrode and furthermore is infrequently reported due to the challenges in achieving lean operation in coin cells.[16] As the redox chemistry happens during sulfur and LiPS conversion, which partly occurs in the liquid phase, the electrolyte in the LELSB encounters problems that are not the case in Li-ion battery systems. For example, the shuttle effect of LiPS significantly affects the cycling performance and rate capability, mainly due to the inventory loss of electrode materials and conductivity decline after cycling.[21] This remains a major barrier to reaching the high theoretical capacity (1670 mAh g^{-1}_s). In addition to the well-known shuttle effect, the liquid system also suffers from dynamic SEI instability,[22] dendritic lithium regrowth,[23] uncontrolled Li_2S precipitation,[24] and electrolyte degradation[25]—all of which contribute to rapid performance decay, particularly under lean-electrolyte and high-loading conditions,[26] thus limiting practical application. The side effects of low E/S ratio, high lithium salt concentration and high sulfur loading are shown as the increased viscosity of the electrolyte,

which poses significant limitations on ionic transportation, polysulfide diffusion and electrodes interfacial kinetics.[27,28]

2.2. Mechanism

Multiple chemical reactions are involved during the charging and discharging process of LELSBs, which gives rise to the characteristic 'two plateau' shape shown on the voltage versus capacity graph (Figure 1a). Each plateau is attributed to the formation of a range of sulfur species of varying solubility in the liquid electrolyte.[32–34] The multi-step conversion between sulfur and Li_2S dominates the mechanism, mediated by a series of LiPS during the charging and discharging processes.[35]

The solid sulfur is converted into Li_2S during the discharging process, where sulfur is reduced at the positive electrode into long-chain LiPS (i.e. Li_2S_8, Li_2S_6), which can be dissolved and then travel in the electrolyte.[36] According to the solution-mediated reaction mechanism, the long-chain LiPS are further reduced to shorter-chain LiPS (i.e. Li_2S_4, Li_2S_2), and finally to insoluble Li_2S, which precipitates on the positive electrode surface[37] (**Figure 4b**). Despite the numerous mechanisms proposed to date, the most widely acknowledged mechanism is that the lithium negative electrode plays an important role in releasing Li-ions into the electrolyte for reaction with sulfur by being oxidized.[38]

During the charging process, insoluble Li_2S at the positive electrode is oxidized stepwise back to short-chain and then long-chain LiPS, eventually reforming solid elemental sulfur. Meanwhile, Li-ions generated from the stepwise oxidation of LiPS species at the positive electrode diffuse through the electrolyte and are subsequently reduced at the negative electrode, leading to the deposition of metallic lithium.[39]

The multistep reaction chain shows the formation of the final product Li_2S from solid sulfur by obtaining electrons, which leads to difficulties regarding LiPS.[40] The LiPS generated from solid sulfur at the positive electrode can dissolve in liquid electrolyte and diffuse to the negative electrode, where it reacts and is deposited as unevenly-distributed Li_2S solid, which is an insulator and hinders the movement of Li-ions[41] (Figure 3a iii). This phenomenon leads to a decrease in active surface area and irreversible consumption of lithium, electrolyte, and sulfur materials. The reactions between LiPS, lithium and electrolyte yield not only liquid and solid products, but also gaseous species.[42] The solid products Li_2S and Li_2CO_3 will be deposited on the negative electrode to form the SEI (Figure 3a iii).[43] During cycling, the formation and accumulation of liquid-phase byproducts such as LiPS may alter the electrolyte composition, thereby reducing the ionic conductivity and degrading overall performance. The gaseous products will be presented as bubbles, which gather around the electrode surface and electrolyte to increase the internal resistance, which will further hinder the transportation of ions.[31,44]

2.3. Function and Mechanism of $LiNO_3$

The incorporation of $LiNO_3$ as an electrolyte additive in liquid-electrolyte Li–S cells has been widely adopted (used by 73% of samples in a recent meta-analysis)[16] due to its profound impact on mitigating the detrimental polysulfide shuttle effect and stabilizing the lithium metal negative electrode, thereby improving rate capacity and prolonging cycling life. The beneficial effects of $LiNO_3$ were first systematically investigated by Aurbach et al.,[45] who demonstrated that $LiNO_3$ promotes the in situ formation of a stable and passivating SEI covering the Li metal surface via the spontaneous redox reaction between NO_3^- and Li metal, thus physically suppressing the electrolyte and lithium salts from further decomposition by accepting electrons on the Li negative electrode surface, which supresses uncontrollable, irreversible side reactions and improves the coulombic efficiency.[46] The SEI layer, primarily composed of inorganic chemically stable products such as LiN_xO_y and Li_xNO_y (Figure 3b vii), functions as an electronically insulating yet ionically conductive barrier that prevents lithium metal corrosion caused by continuous reduction of dissolved LiPSs at the Li negative electrode interface, a key source of inefficiency in liquid-phase Li–S batteries.[45,47]

Mechanistically, the role of $LiNO_3$ as an electrolyte additive has been attributed to its preferential electrochemical reduction on the lithium surface ahead of LiPS, which means that chemically stable products can favorably occupy the surface of lithium as SEI (Figure 3b vii), thereby blocking the further transfer of electrons to solvent molecules and LiPS.[48,49] Utilizing the combination of X-ray photoelectron spectroscopy (XPS) and time of flight secondary ion mass spectrometry (ToF-SIMS) researchers have confirmed the formation of surface species such as Li_3N and LiN_xO_y after cycling in the electrolyte with $LiNO_3$ added (Figure 3b vii), which shows the formed species can not only contribute to reinforce the chemical robustness of the system by forming the SEI but also participate in modulating the lithium deposition morphology and promote uniform growth.[50,51]

The effect of $LiNO_3$ is not limited to the lithium negative electrode surface, as it also influences the redox behavior of LiPS in the electrolyte. Zhuang et al.[52] showed via operando UV–vis and electrochemical impedance spectroscopy (EIS) that $LiNO_3$ alters the speciation of dissolved LiPS, indicating the shorter-chain species can exhibit lower solubility, thus lower diffusivity, thereby reducing the extent of shuttle-driven losses (Figure 3b iv). Zhang et al.[53] demonstrated that $LiNO_3$ assists the conversion of soluble long-chain LiPS back to elemental sulfur deposited in the positive electrode matrix at the end of the charging process, which significantly suppresses the redox shuttle effect. These studies demonstrate that $LiNO_3$ plays an integral role in mediating interfacial stability across both electrodes, which ensures more complete utilization of active material by closing the polysulfide redox loop.

Despite the advances to date, the specific chemical nature, dynamic evolution, and spatial heterogeneity of the $LiNO_3$-derived SEI remain the subject of ongoing debate. In particular, the influence of electrolyte composition, cycling protocol, and temperature on SEI composition and mechanical integrity is insufficiently understood. As highlighted by Zhang et al.,[54] real-time *operando* characterization, such as cryogenic transmission electron microscopy (cryo-TEM) and in situ XPS, are essential for unravelling the morphological evolution of the SEI and understanding how $LiNO_3$ decomposition products are incorporated into the interphase structure. Given the central role of $LiNO_3$ in the conventional LELSB configuration, resolving these

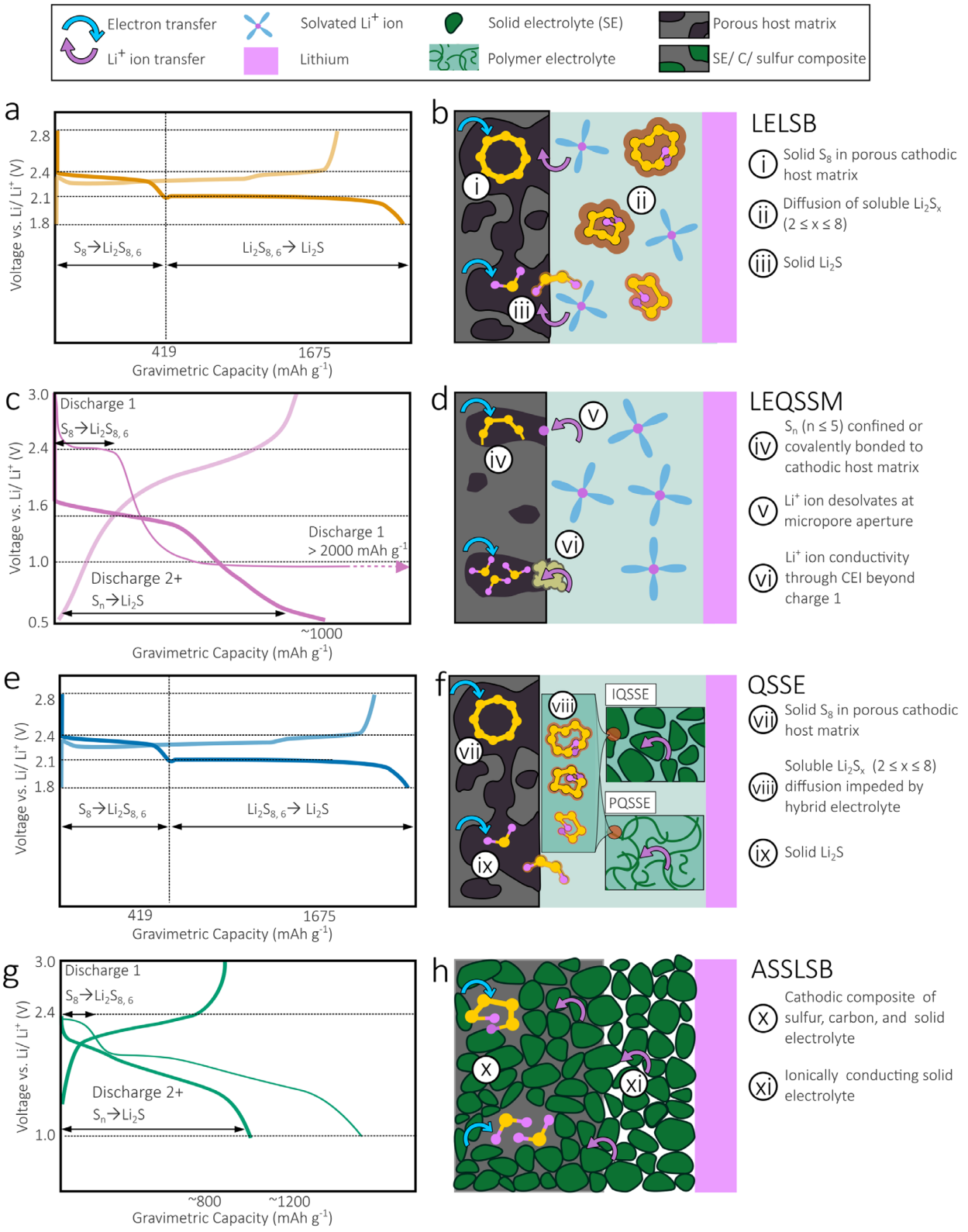

Figure 4. Overview of capacity voltage profiles and conversion chemistry mechanisms in (a,b) liquid electrolyte Li-S battery (LELSB), (c,d) Li-S battery with liquid electrolyte and quasi-solid state conversion mechanism (LEQSSM), (e,f) Li-S battery with hybrid quasi-solid state electrolyte with inorganic component (IQSSE) or gel-like polymer (PQSSE), and (g,h) all-solid-state Li-S battery (ASSLSB). Schematics illustrate discharge proceeding from top to bottom of each sketch.

mechanistic issues will be vital to further advances in both electrolyte formulation and negative electrode protection strategies.

2.4. Limitation of $LiNO_3$-Based system

Although $LiNO_3$ is widely adopted in the literature, its application is mainly constrained by irreversible consumption, limited solvent compatibility and safety concerns. One of the most critical limitations lies in the irreversible consumption of $LiNO_3$ during cycling. As the electrolyte undergoes one-way electrochemical reduction at the lithium surface to form a protective SEI, the resulting interphase is initially effective at suppressing parasitic polysulfide reactions but is not regenerable under conventional operating conditions. Mikhaylik and Akridge first reported that the protective effects of $LiNO_3$ diminish over prolonged cycling, with a progressive breakdown of the SEI exposing the lithium negative electrode to continuous reduction by soluble LiPS and reactivating the shuttle effect.[21] To address this, various strategies have been explored, such as incorporating redox mediators that regenerate $LiNO_3$-like species in situ, or engineering electrolyte reservoirs that continuously supply $LiNO_3$ throughout extended operation.[55] Although redox mediators have been shown to promote polysulfide conversion and improve reaction kinetics, their contribution is often contingent upon the positive electrode's intrinsic electrochemical performance and structural design.[56–58] In the absence of a robust conductive framework and effective active site utilization, the benefits of redox mediators remain limited. Moreover, both the use of an excess reservoir of $LiNO_3$ and auxiliary methods of periodic replenishment will impose (potentially quite severe) penalties on energy density and system design. Zhang et al.[54] demonstrated that the combination of a soluble nitrate in the electrolyte and an insoluble nitrate in sulfur positive electrode can generate a synergetic effect as soluble nitrates act quickly but deplete fast, while insoluble nitrates offer slower yet longer-lasting protection. NO_3^--based additives not only stabilize the SEI but also suppress LiPS shuttling by redistributing charge at the Li surface, increasing the overpotential for interfacial reactions and slowing parasitic kinetics of LiPS. Additionally, recent studies have examined the synergy between $LiNO_3$ and solvent systems, particularly ether-based electrolytes such as DOL/DME, demonstrating that the stability of the SEI and solubility of LiPS can be simultaneously modulated through tailored solvent–additive interactions.[59] However, the proposed synergy between soluble and insoluble nitrates hinges on a delicate balance in concentration and spatial distribution, which is difficult to maintain in practical cells, especially under lean electrolyte or high-loading conditions. Therefore, despite the promising functionalities of $LiNO_3$-based strategies, their practical implementation necessitates a more comprehensive understanding of the spatiotemporal evolution of interfacial chemistries, dynamic electrolyte–electrode interactions, and overall compatibility with other cell components under realistic operating conditions.

Moreover, $LiNO_3$ additive depletion can lead to both chemical and mechanical instability of the SEI produced by LiNO3-initiated reactions. Although the SEI formed initially provides an electronically insulating but ionically conductive barrier, its structural fragility under conditions involving non-uniform lithium plating and high current densities reduces stability over long-term cycling (Figure 3aiii). Previous studies on cryo-TEM and focused ion beam-scanning electron microscopy (FIB-SEM) have revealed that $LiNO_3$-induced SEIs are prone to cracking, delamination, and inhomogeneous growth during charging and discharging, which lead to dendrite nucleation, accelerated capacity fade and even localized short circuits.[60,61] As demonstrated by Zhang et al.,[62] the chemical composition of $LiNO_3$-induced SEI evolves dynamically over its life span, as the sulfur-containing species such as Li_2SO_3 and Li_2SO_4 are susceptible to further reduction or dissolution under fluctuating redox chemical conditions. The interfacial instability of SEI indicates that the generation of SEI induced by $LiNO_3$ lacks the robustness and resilience needed for long-term cycling applications, especially under lean-electrolyte or high sulfur loading configurations.

$LiNO_3$ also suffers from its narrow solubility window and high concentration sensitivity in common ether-based solvents system. In the commonly used DOL:DME systems, the saturation concentration of $LiNO_3$ is typically below 0.5 M[63] (**Figure 5**). Insufficient concentrations of the additive will result in incomplete passivation of the lithium surface, allowing for continued parasitic reactions, while excessive concentrations can lead to increased viscosity, suppressed ionic conductivity and induced interfacial polarization.[64] High concentrations of $LiNO_3$ have been shown to introduce additional oxidative instability at the positive electrode side, where nitrate anions may undergo unwanted redox reactions with sulfur species or electrolyte solvents in cells operating above 2.5 V, leading to the formation of resistive interfacial films.[65] In high cell-level energy configurations with thick sulfur positive electrodes or low electrolyte volumes, formulation accuracy is critical, and the margin of error for additive loading is very small, which leads to many practical problems.

From the perspective of electrolyte design, the poor solvent compatibility of $LiNO_3$ is also an important bottleneck. It has poor solubility in non-ether solvents (such as carbonates, fluorinated ethers, and ionic liquids) and has limited utility in systems that seek higher thermal stability or non-flammability. For example, carbonate electrolytes are often used in high-voltage Li-ion batteries due to their good electrochemical stability, but $LiNO_3$ is not compatible with them because of its poor solubility and tendency to undergo side reactions[55] (the use of carbonate-based solvents in $LiNO_3$ free Li-S cells is discussed further in Section 3). This not only limits the applicability of $LiNO_3$ in multicomponent electrolyte formulations but also exacerbates the difficulty of balancing the volatility, safety, and interface performance of electrolytes.

In addition to performance and formulation limitations, $LiNO_3$-based systems also face significant safety issues. As a strong oxidant, $LiNO_3$ has potential thermal and chemical hazards under abuse conditions (such as overcharging, short circuiting, or high temperature). Differential scanning calorimetry (DSC) and accelerated rate calorimetry (ARC) studies have shown that $LiNO_3$ can react exothermically with common battery components (especially polyolefin separators and polymer binders) at temperatures as low as 130 °C.[59] These reactions may release flammable NO_x gas, further exacerbating the risk of thermal runaway and posing challenges to thermal

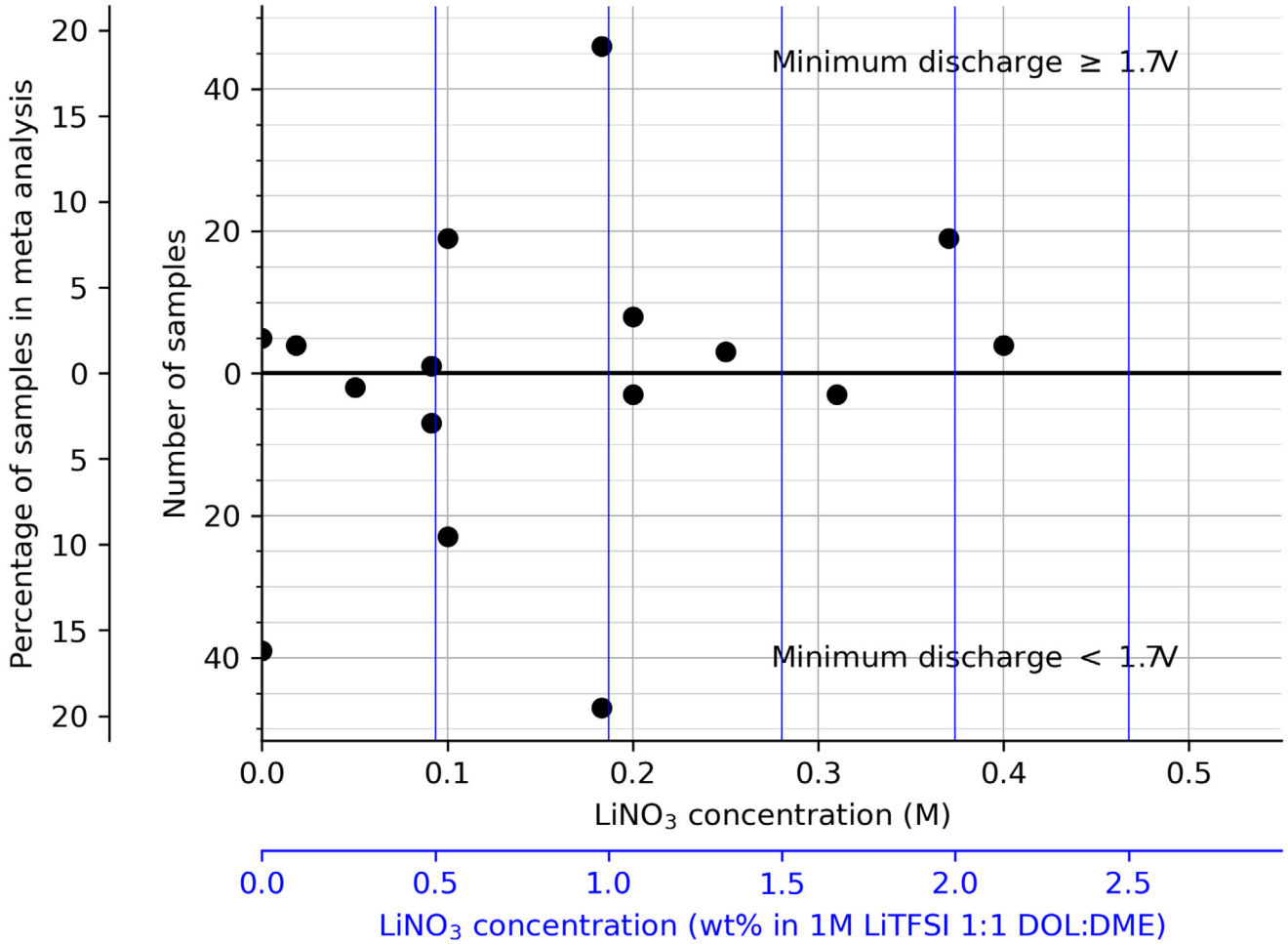

Figure 5. Frequency of reporting of $LiNO_3$ electrolyte concentration in 264 samples reported in 100 articles, separated into samples with minimum discharge voltage cutoff ≥1.7 V (upper half of axes) and <1.7V (lower half of axes). Horizontal axes show $LiNO_3$ concentration (converted to molality using reported $LiNO_3$ and LiTFSI concentration where originally reported as wt.%); vertical axis shows number of samples using the indicated $LiNO_3$ concentration and voltage cutoff range, with offset axis showing relative frequency within meta-analysis study. For example, 19 samples report the use of 0.1M $LiNO_3$ combined with a minimum discharge voltage ≥1.7 V. Data from.[16]

management and safety certification, especially in large-scale battery applications such as electric vehicles and grid energy storage.

Fundamentally, the limitations of $LiNO_3$ reflect a deeper problem of the LELSB system: soluble LiPS and highly reactive lithium metal make the system intrinsically unstable. In this context, LEQSSM, QSSE, and ASSLSB systems are expected to alleviate these core problems through fundamental structural changes. Solid electrolytes can limit the diffusion of LiPS and physically isolate the lithium negative electrode, thereby inhibiting the shuttle effect and improving battery safety.

2.5. Summary

As a more mature electrolyte system in terms of mechanistic understanding, LELSB have made notable strides over the past few decades in improving energy density and cycle life. However, it still faces persistent challenges arising from the inherent instability and complexity of the energy storage mechanism imposed by its redox chemistry. Alongside efforts to optimize electrolyte formulations, improving the structure and composition of the positive electrode has emerged as a major focus for the future. This, in turn, places greater demands on our understanding of the interfacial mechanisms between the electrolyte and the electrodes—particularly given the ongoing debate around the precise chemical composition, dynamic evolution, and spatial heterogeneity of the SEI derived from $LiNO_3$.

$LiNO_3$ has long been widely employed in LELSB to stabilize the negative electrode and suppress polysulfide shuttle effects, contributing to improved cell performance. However, it must be recognized that the functionality of $LiNO_3$ additive is highly dependent on its concentration in the electrolyte which gradually diminishes as it is consumed during cycling. In addition, the intrinsic oxidative nature of $LiNO_3$ raises safety concerns, posing a critical challenge that must be addressed for the practical deployment of Li–S batteries across diverse application scenarios. As such, efforts to simultaneously enhance the performance of LELSB while

improving safety and scalability have driven the exploration of alternative electrolyte configurations. Although LEQSSM, QSSE, and ASSLSB systems still face challenges in interface engineering and ion transport (Figure 2), their potential to overcome the bottleneck of liquid phase systems has been initially demonstrated. Liquid, quasi-solid state, and solid-state Li–S batteries should be regarded as complementary technical routes. Liquid systems exhibit comparatively high rate performance and manufacturing maturity, while solid-state designs may offer enhanced safety and cycle life (see Figure 2) when compared to the alternative cell formats discussed in this work; however further development across the cell is undoubtedly required to enable practical deployment in the field. As outlined previously, this includes the removal of $LiNO_3$, which has historically been widely deployed to mitigate the effects of polysulfide shuttle. To achieve this, alternative strategies must be considered, which may include physical mitigation in the form of separator design or isolation of the Li-metal anode using protective layers.[66,67] Further research into additives which may promote the reduction of the polysulfides may also enable more control on the discharge pathways, perhaps avoiding the formation of Li_2S_6 in doing so, chemically or catalytically mediating shuttle.[58,68] These approaches would remove the most critical degradation pathway in the cell by mitigating material loss to the negative electrode, with the promise of extended lifetimes offered; however, they are highly likely to add additional mass and cost to the cells. Incorporating solvents with Li-passivating and/or shuttle mitigating functionality is also likely to support extended lifetimes, with highly fluorinated solvents offering some promise in this regard. The fundamental mechanism also places a minimum on the electrolyte volume, which must be used to avoid excess viscosity, whilst enabling full wetting of the positive electrode, impacting performance. Given that the electrolyte can provide 40–60% of the mass of the cell identifying routes to achieve close to this minimum level through minimization of the porosity of the positive electrode, and optimization of the electrolyte properties is also likely to provide significant benefits to the commercial prospects of the cell.

Ultimately, to truly unleash the potential of Li–S technology, it is necessary to achieve synergistic progress in interface design, electrolyte chemistry, and battery structure and leverage developments in complementary cell types to accelerate the development of the chemistry as a whole. This cell format is undoubtedly the most heavily researched and, by extension, the most mature of those considered in this work. As a result, it is likely that early Li-S cells in the field will operate via this mechanism; however, as the technology matures, the mechanistically imposed restriction on the gravimetric energy density is likely to drive interest towards cells in which the sulfur is physically constrained in the positive electrode and operates using a 'more' solid-state type mechanism.

3. Liquid Electrolyte with Quasi-Solid-State Conversion Mechanism

The distinction between hybrid Li-S cells utilizing a quasi-solid-state electrolyte, comprising a minimal amount of liquid electrolyte added to a solid electrolyte, and Li-S cells using a liquid electrolyte to achieve a solid–solid conversion of the sulfur to Li_2S, has been drawn in Section 1. The former configuration, referred to as QSSE cells, will be discussed in Section 4, while this section focuses on the latter. In the Li-S system, there are also entirely liquid electrolytes that can achieve the quasi-solid state conversion process of sulfur by limiting or eliminating the formation of soluble LiPS (Li_2S_n $2 \leq n \leq 8$). This LEQSSM mechanism avoids the capacity degradation related to inventory loss and the LiPS shuttle effect seen in the LELSB mechanism with liquid electrolyte discussed in Section 2, while the liquid electrolyte avoids challenges related to charge-transfer resistance at the electrolyte-electrode interface affecting ASSLSBs (see Section 5). In LEQSSM systems, the active material is confined to the positive electrode structure by means including confinement in micro pores, covalent bonding between sulfur species, electrically conducting cathodic host matrix, and the use of sparingly solvating electrolytes.[69] The imposition of this alternative operating mechanism also offers the possibility for reduced electrolyte volumes, as there is no need to accommodate significant viscosity variations associated with LiPS dissolution as the cell discharges. This lower loading offers either a tangible route to improved energy density, with the electrolyte in conventional cells comprising up to 50% of the mass of the cell,[1,18,70] or the potential to reduce the sulfur loading in the positive electrode and achieve a similar energy density to a conventional cell. This reduction in the requirement for ultrahigh sulfur loadings, in principle, allows for a wider design window for the positive electrode and the targeting of application-specific designs for energy, rate and lifetime focused cells.

3.1. Steric Confinement by Micropores and Cathode-Electrolyte Interphase

One route to the LEQSSM conversion mechanism involves confining the active material to the positive electrode matrix by physical confinement in micropores or by covalent bonding. In these systems, the reversible conversion reaction may terminate in short-chain sulfur molecules[71–75] rather than S_8, denoted as S_n ($n \leq 4$) throughout this section. This process is characterised by a single voltage plateau during discharge[71,73,76] at 1.6–1.85 V vs. Li/ Li^+, associated[77] with the reduction of confined S_2, however as shown in Figure 4c, the wider voltage stability of electrolytes compatible with LEQSSM systems offsets decreased energy density.

By combining a microporous conductive host matrix with a suitable electrolyte, S_n molecules can undergo conversion to Li_2S in isolation from the electrolyte solvent, thereby avoiding soluble LiPS formation and diffusion. This mechanism permits reaction between desolvated Li^+ ions and S_n species while preventing contact between the solvent and the active material via steric hindrance due to the small pore diameter (Figure 5ai),[76,78,79] and by forming an ionically conductive positive electrode (cathode)-electrolyte interphase (CEI) at the pore opening to serve as a barrier between the solvent and active material (Figure 5biii). Sulfur may be infiltrated into microporous hosts by heating at temperatures exceeding the commonly-used 155 °C used for mesoporous host matrices,[16,80] resulting in short-chain allotropes[71–73] of sulfur S_n ($1 \leq n \leq 5$). Microporous host matrices have a smaller specific pore volume than mesoporous materials, resulting in lower total sulfur loading in the electrode and limiting the cell's

Table 1. Comparison of performance and parameters for LEQSSM Li-S cells with microporous carbon and covalently bonded SPAN electrodes.

Positive Electrode	Sulfur loading (mg cm^{-2})	Electrolyte Solvent	Initial Capacity (mAh g^{-1}_s)	End of Life Capacity (mAh g^{-1}_s) (cycles)	Highest C-rate reported	Reference
S: C: PTFE: MWCNT = 22:63:12:3	1.7 ± 0.2	30 µL of 1M $LiPF_6$ in EC/DMC v:v = 1:1	420	224 (200)	0.1	[72]
S: CNT+C: PVDF: CB = 32: 38: 10: 10	n.d.	1M $LiPF_6$ in EC/DMC v:v = 1:1	668	457 (200)	5	[71]
S: C: CB: SA = 22 :48: 15: 15	0.17	100 µL of 1M $LiPF_6$ in EC/DMC v:v = 1:1	660	630 (4100)	6	[73]
S:C@ CB: PVDF = 16:64:10:10	n.d.	1M $LiPF_6$ in EC/ DMC/ EMC v:v = 1:1:1	1070	885 (50)	1.8	[76]
S: C: CB: SA = 14: 56:15 :15	0.08-0.14	1 M $LiPF_6$ in EC/DMC v:v = 1:1	250	102 (1600)	0.89†	[77]
S: C: CB: PVDF = 48:32:10:10	0.71 – 0.91†	0.5 M Li FSI in MPP FSI IL	1678	1005 (55)	0.03†	[78]
(S:C):AB: PVDF-HFP = 8:1:1	1.2	1 M LiPF6 in EC/DEC/FEC v/v/v = 4:4:2	1190	880 (300)	0.19†	[84]
S:C = 1:1	4.23	1 M $LiPF_6$ DMC/FEC v/v = 4:1	1250	680 (100)	0.1	[86]
S:CB:PVDF = 8:1:1	1.2-1.4	1M LiTFSI in DOL/DME v:v = 1:1 with 1 wt% $LiNO_3$	939	731(150)	2	[89]
41 ± 1 wt% sulfur in SPAN (precursor S:CB:PVDF = 7:1.5:1.5)	n.d.	1M $LiPF_6$ in EC/DMC/DEC w:w:w = 50:25:25	487 mAh $g^{-1}_{cathode}$	260 mAh $g^{-1}_{cathode}$ (40)	0.1	[94]
41 wt% sulfur in SPAN (SPAN: CNTs 88:12)	4	30 µL of 1M $LiPF_6$ in EC/ DMC/ EMC v:v:v = 1:1:1	400	1170 (800)	0.96†	[93]
37.57 wt% sulfur in SPAN	n.d.	1M LiTFSI DOL/ DME v:v = 1:1 with 0.2 M LiNO3	1225	1185 (500)	0.96	[95]

AB = Acetylene black, DEC = diethyl carbonate, DMC = dimethyl carbonate, EC = ethylene carbonate, EMC = ethylmethyl carbonate, FEC = fluoroethylene carbonate, IL = ionic liquid, LiTFSI = bis (trifluoromethane) sulfonamide lithium salt, MPP = methylpropyl pyrrolidinium, PVDF-HFP = poly(vinylindene fluoride-coo-hexafluoropropylene), SA = sodium alginate. †Inferred from reported values (not reported in units used here)

maximum gravimetric capacity.[81] On the other hand, the direct electrical contact between the conductive host and the insulating active material facilitates long-term capacity stability[69] (see **Table 1**)

The LEQSSM system requires electrolyte solvents with low solubility for LiPSs, by contrast to the ether-based electrolyte solvents used in LELSBs (see Section 2). Carbonate-based electrolyte are incompatible with conventional solid–liquid–solid Li-S conversion due to the low solubility of LiPSs and their degradation via nucleophilic reaction between the solvent and LiPSs,[82] however, when used with confined solid S_n/Li_2S, carbonate-based electrolytes contribute to the formation of functional passivating layers on both the negative electrode and positive electrodes. For the former, the use of fluoroethylene carbonate (FEC) improves the Coulombic efficiency of lithium metal negative electrodes by promoting uniform deposition of lithium during charging, enabled by a stable passivating layer with high ionic conductivity.[83,84] As an example of the latter, Wang *et al.*[77] used an ultramicroporous carbon (0.5 nm pores) in conjunction with 1:1 ethylene carbonate (EC): dimethyl carbonate (DMC) solvent with $LiPF_6$ salt to form a CEI dominated by lithium ethylene monocarbonate (LEMC) and lithium methyl carbonate (LMC) (see **Figure 6**): commercial Li-ion cells use the same electrolyte composition and form SEI with the same composition, albeit via a different decomposition mechanism. However, Kensy et al.[72] demonstrated that only carbon hosts with sufficiently small diameters (*ca.* 0.7–2 nm) were compatible with the formation of a CEI that effectively encapsulated the S_n while admitting Li^+ ions, while complete encapsulation was not realized in pores with larger diameters in combination with the same electrolyte and voltage conditions. This is consistent with the micropores (<2 nm,[85]) and sub-nanometre pores reported in other examples[71,73,78,84,86] of single voltage plateau LEQSSM conversion. Therefore, the quasi-solid state sulfur conversion mechanism in liquid electrolyte is facilitated by the combined properties of the cathodic host matrix properties and the electrolyte composition.

Micropores with openings ≈1 nm may limit the sulfur molecule length S_n and exclude the formation and diffusion of soluble long-chain LiPS, however it is likely that it is the confinement of S_n and its isolation from solvent molecules,[78] rather than short molecular chain length, that determines the LEQSSM conversion.[69] The formation of the CEI and solid-solid conversion of S_n to Li_2S confined within micropores is further demonstrated by operando small angle neutron scattering (SANS) and X-ray diffraction (XRD) data acquired by Senol Gungor et al.,[86] where initial changes in peak intensity indicate changes in the contents of micropores which then remain stable during subsequent cycles, without the formation of additional SANS peaks associated with the formation of additional deposits beyond the micropores. This confinement mechanism is supported by the findings of by Markevich et al.,[78] who confined sulfur in microporous carbon (≤ 2nm diameter pores) and tested the electrodes in ionic liquid (IL), polycarbonate (PC) based, and conventional ether-based electrolyte solvents, comparing electrodes with and without pre-treatment in the IL with FSI^- electrolyte salt to form a CEI. A single plateau LEQSSM discharge profile was possible in the ether-based electrolyte only after pre-forming the CEI.

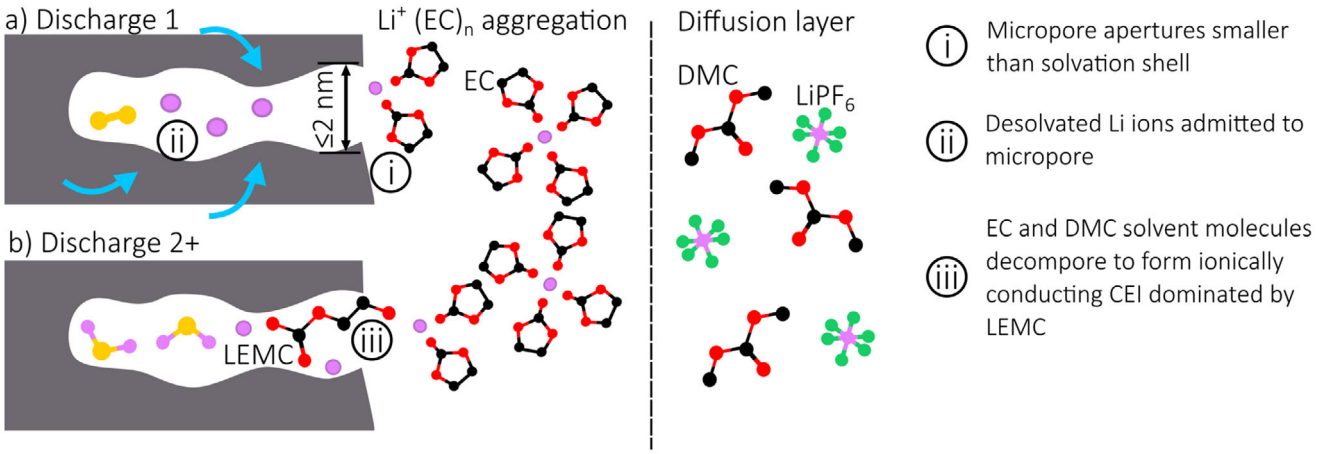

Figure 6. Schematic diagram of CEI formation in micropore opening during the first cycle (a) and following carbonate electrolyte decomposition during the first discharge cycle (b). After Wang et al.[77]

Similarly, Li *et al.*[84] demonstrated LEQSSM conversion of microporous confined sulfur using a carbonate electrolyte, although here the passivating layer was deposited prior to electrolyte decomposition by the deposition of alucone via molecular layer deposition (MLD).

Functionalization of the carbon framework with heteroatoms can increase the electrical conductivity of the host matrix, increase the binding energy between the active material and host matrix, and reduce the barrier to electron transfer to the active material, thus improving reaction kinetics.[87,88] For example, Niu et al.[89] utilized a nitrogen-doped microporous carbon host matrix with a carbonate electrolyte and demonstrated faster kinetics through higher capacity retention at high rate and lower charge transfer resistance from EIS (645 vs. 390 mAh g^{-1}_S at 3C, and 30.5 Ω versus 62.8 Ω for electrodes with and without nitrogen doping, respectively). Li et al.[90] developed a nitrogen-doped microporous carbon that exhibited a stable capacity of 902 mAh g^{-1}_S at 0.2 C and an excellent rate capacity of 511.8 mAh g^{-1}_S at 10 C after 500 cycles in a carbonate electrolyte. It also demonstrated good compatibility with ether-based electrolytes.

3.2. Confinement by Covalent Bonding

When synthesizing Li-S positive electrodes compatible with the solid-solid conversion mechanism in liquid electrolytes, an alternative to the physical confinement of sulfur in micropores is covalently bonding the sulfur to the conductive host matrix. Sulfurized polyacrylonitrile (SPAN) can be synthesized via the vulcanization of polyacrylonitrile (PAN), resulting in the formation of organosulfide groups including C—S, cross-linked S-S_n-S, and side-chains with length S_n (typically $n \leq 5$).[91] Possible mechanisms for solid-solid S_n–Li_2S conversion pathways are shown in **Figure 7**, where aromatically bound C—S (A), 'bridging' C—S_n (B), non-aromatic C—S and C═S (C), and side-chain S_n (D) moieties are shown. Li-S cells with SPAN positive electrodes typically utilize carbonate-based electrolyte[92] solvents to mitigate the formation of soluble LiPS and thereby prevent diffusion-related capacity degradation, which may occur due to residual S_8 following synthesis or due to electrochemical generation of S_8 during discharge when using ether-based solvents with high sulfur and LiPS solubility.[93] As shown in Figure 4d, the first discharge cycle may have an irreversible capacity exceeding the theoretical gravimetric capacity of sulfur, attributed to the ionic bonding[84] (Figure 7D) or co-ordination (Figure 7 A–C) of Li^+ ions to the aromatic N sites.[93] In subsequent cycles, the remaining capacity is associated with the reversible conversion of sulfur moieties to form nanosized Li_2S aggregates within the fibrous SPAN network.[93] Despite the low first-cycle Coulombic efficiency, these reversible reactions have a lower overpotential than the initial reaction (with a discharge voltage plateau around 1.9V vs. Li/ Li^+), and the absence of inventory loss due to soluble LiPS diffusion means that cells with SPAN positive electrodes show long-term cycling stability (see Table 1with examples).

The sulfur content is determined by factors including the processing temperature and PAN molecular weight, and to a lesser extent by the pressure used and duration of vulcanization,[92] and is limited to c 42 wt.%[91,94] (see Table 1), therefore posing similar challenges to the low maximum sulfur content possible, and by extension practical cell energy density, to the microporous carbons discussed above. However, the electrical conductivity and mechanical structure of SPAN can enable the synthesis of self-supporting electrodes and avoid the requirement for current collectors and minimize the use of conductive additives and binders, thereby improving the cell-level gravimetric capacity. The benefit of these self-supported electrodes, while discussed in the literature, poses challenges when scaled to a commercially relevant cell scale, which may render them theoretical. Li et al.[95] demonstrated the use of electrospinning of a composite of PAN and carbon nanotubes (CNTs) followed by sulfurization to attain a capacity of 1280 mAh g^{-1}_S after 200 cycles at 400 mA g^{-1}_S (c. 0.24 C), with an optimized sulfur loading of 38 wt.% sulfur as measured by energy dispersive X-ray spectroscopy (EDX). SPAN-based electrodes with enhanced electrical conductivity have been attained by using S_xSe_{1-x} compounds,[96,97] however, as Se also participates in the Li^+ storage mechanism these compounds are beyond the scope of this review.

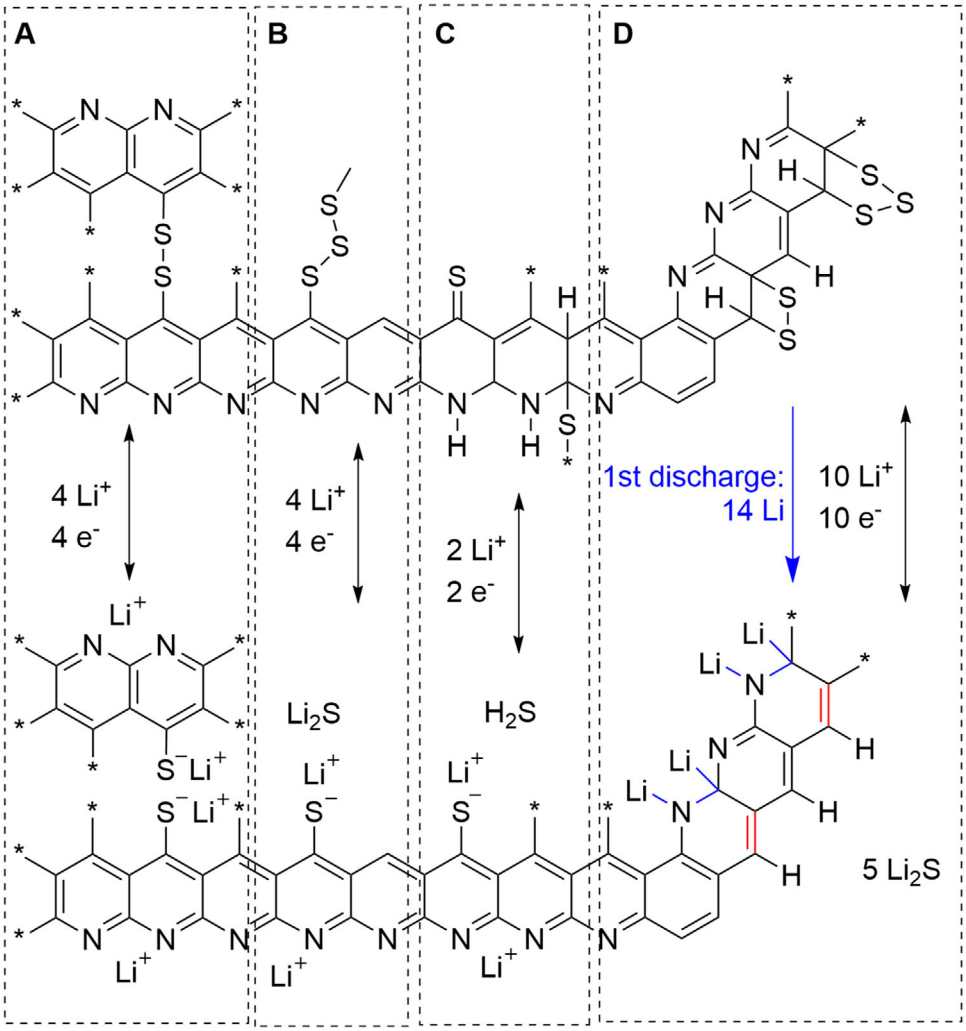

Figure 7. Summary of sulfur – Li_2S conversion mechanisms in SPAN. Sulfur moieties from,[94] A—C) after,[93,104–106] D) after.[93,104–106]

The cathodic host matrices discussed in this review typically refer to microporous carbon, since they provide electrical conductivity while remaining lightweight to complement the high energy density of sulfur. Alternatively, sulfur may be incorporated into sulfur-rich metal polysulfides, using metal anions with high coordination ability, including Mo,[98] Ti,[99] Fe,[82] Ni,[100] and Cu.[101] A common feature of these materials is that they have an amorphous structure consisting of chains of LiPS connected by metal linkers. The metal linkers connect the short sulfur chains like tentacles, preventing the formation of soluble long-chain LiPS during battery cycling.[102] For example, Li et al.[82] demonstrated that structure-oriented electrochemical reaction mechanisms/pathways for sulfur negative electrodes expand the possibilities of sulfur-based positive electrodes in carbonate electrolytes by introducing Fe atoms, which prevents the formation of long-chain LiPS, thereby enabling lithiation/de-lithiation pathway switching of sulfur positive electrodes in LEQSSM systems. However, the active participation of the metal heteroatoms in the Li^+ storage mechanism is distinct from the sulfur conversion outlined in Figure 4e, leading Ye et al.[103] to propose categorizing them as "sulfur-equivalent positive electrode materials", and as such, a detailed discussion of the conversion mechanism of these metal polysulfide positive electrodes is beyond the scope of this review.

3.3. Electrolytes with Limited Solubility

An alternative strategy to moderate the dissolution of S_n by using a sparingly solvating electrolyte was demonstrated by Pang et al.[107] using a 'solvent-in-salt' electrolyte containing diglyme and LiTFSI in a 0.8:1 ratio by mass. By adjusting the salt concentration, they attained a single voltage plateau discharge mechanism for diglyme: LiTFSI ratios below ≈1:1. By contrast to the microporous confinement mechanisms discussed previously, this was attributed to the solid–solid conversion enabling particle-like deposition of Li_2S, thereby preventing pore network blocking, and the formation of a dense, thin SEI on the lithium negative electrode (discussed below). This electrolyte system can be referred to as a high-concentration electrolyte (HCE). Similarly, systems capable of achieving solid or quasi-solid state conversion of sulphur using liquid electrolytes include the following:

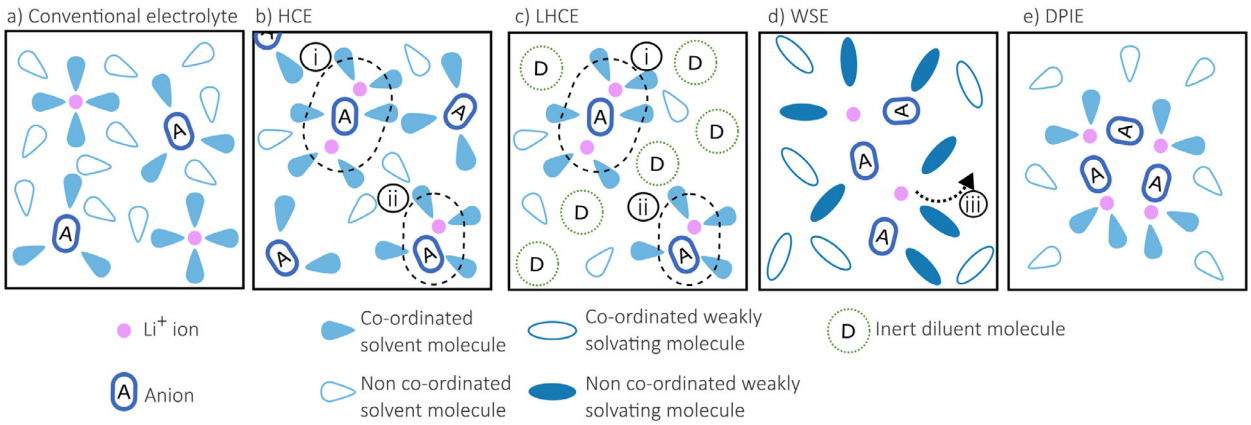

Figure 8. Schematics representing Li^+ ion, electrolyte salt anion, and solvent molecule configurations in different electrolyte systems: a) conventional liquid electrolyte (LELSB), b) highly concentrated electrolyte (HCE), c) localised high concentration electrolyte (LHCE), d) weakly solvating electrolyte (WSE), and densely packed ion cluster electrolyte (DPIE). Highlighted mechanisms include i) aggregates, ii) contact ion pairs, iii) Li^+ ion transfer. After.[107–112]

localized high-concentration electrolytes (LHCE), weakly solvated electrolytes (WSE), and densely packed ion cluster electrolytes (DPIE). Each electrolyte utilizes a unique solvation structure: HCE (the 'solvent-in-salt' system) contains a large amount of salt, causing Li^+ to be strongly coordinated by anions (forming contact ion pairs and aggregates), thereby suppressing the solubility of free solvent and polysulphides (**Figure 8b**). LHCE dilutes HCE by incorporating an inert solvent ('dilutant'), which does not dissolve Li^+, thereby locally retaining the ion pair network while reducing viscosity (Figure 8c). WSEs use inherently low-donor solvents (e.g., sulfonates, nitriles, weak ethers), causing Li^+ to be primarily coordinated by anions, resulting in low LiPS solubility but slower redox kinetics (Figure 8d). Recently, a DPIE has been introduced: mixing a weakly soluble solvent with a diluent forces the formation of dense ion clusters (compact Li^+-anion aggregates) in the bulk phase (Figure 8e). These clusters enable ultrafast Li^+ desolvation and stable interfaces while still suppressing LiPS dissolution. In all cases, the shuttle effect of LiPS is mitigated due to the weakened free solvent environment. These electrolytes not only influence the sulphur conversion process as described above but also affect the voltages of the two platforms, which are typically determined by the solvation free energy of LiPS. The free energy changes from Li^+S to LiPS and from LiPS to Li_2S respectively, determine the first and second plateau voltages. Cui et al.[32] confirmed that 1,1,2,2-tetrafluoroethyl-2,2,3,3-tetrafluoropropyl ether (TTE), as a diluent, weakens the polarisation effect, thereby causing the first plateau to decrease and the second plateau to increase. This trend applies to a series of ether-based electrolytes.

Due to differences in electrochemical behavior, the discharge curves also vary. The conventional LELSB process exhibits a double-plateau curve; the 'solid–solid' conversion always presents a single-slope curve; as for the 'quasi-solid state' conversion, the two plateaus are connected by a segment with a very small slope, forming a curve that is almost a single plateau[69](Figure 4). As discussed in Section 2.2, in LELSBs, the high plateau at c. 2.4V corresponds to long-chain LiPS, while the low plateaus at c. 2.1V corresponds to short-chain LiPS. The voltage relaxation kinetics during the open-circuit voltage (OCV) steady state in Pang et al.'s[107] galvanostatic intermittent titration technique (GITT) study further confirmed the following reactions for the quasi-solid state process of the electrolyte in the diethylene glycol dimethyl ether (G2) system. In the first stage, the main reaction is between S_8 and Li_2S_4, while Li_2S_4 continues to reduce to solid Li_2S in the second stage (see Figure 4c). In this process, S_8 (or other high-order polysulphides) undergoes iterative reduction until it is completely consumed.

3.3.1. High-Concentration Electrolytes

HCEs ('solvent-in-salt systems') employ extremely high salt concentrations (typically >3 M). In Li-S systems, typical examples include LiTFSI present at high concentrations in ether solvents (e.g., DOL/DME). Due to the lack of free solvent, the dominant solvation structures are contact ion pairs (CIPs) and multi-ion aggregates, rather than fully solvated Li^+ (Figure 8bi,ii). These HCEs form robust Li-SEI and CEI layers (due to the dominance of anions near the interface) and severely limit the solubility of LiPS. By increasing the viscosity and reducing the free solvent, HCEs can enhance the cycling stability of cells.[109,113–115] Asano et al.[116] used a weak-solvated electrolyte based on sulfur ether to prevent the dissolution of LiPS, which significantly affected their reversibility. Mikhaylik and Akridge[21] were the first to discover that increasing the concentration of LiTFSI affects the solubility and equilibrium of polysulphides, as well as the viscosity and ionic mobility of DOL/DME-based electrolyte solutions. Using electrolyte solutions with higher LiTFSI concentrations can achieve smaller shuttle constants and lower lithium corrosion rates. Suo et al.[117] found that batteries using a 7 M electrolyte system could still provide high discharge capacity and high coulombic efficiency exceeding 1,000 mAh $g^{-1}{}_S$ but with more severe polarization. Pang et al.[107] revealed the correlation between electrolyte solution concentration, solvent activity, and electrochemical behavior. Increasing the LiTFSI concentration enhances the coordination between TFSI and Li^+. Taking diethylene glycol dimethyl ether (G2) as an example, as the G2:LiTFSI

molar ratio decreases from 7:1 to 1:1, the coordination number of the O atom in $TFSI^-$ in the first Li^+ solvation shell increases from 1 to 2.55, while the free G2 molecules decrease sharply from 71% to 12%. Low solvent activity leads to improved thermal stability and low polysulphide solvation rates. Therefore, at lower G2:LiTFSI ratios, a transition toward a quasi-solid-solid reaction occurs, resulting in a voltage curve approaching a 'single plateau'. However, HCEs still face challenges such as increased viscosity, which may hinder ion migration due to the extensive use of salts.[118]

3.3.2. Localized High-Concentration Electrolytes

LHCEs simulate the solemnization effects of HCE locally while using fewer salts overall. They are prepared by mixing traditional electrolytes (e.g., 1–2 M LiTFSI in DOL:DME) with inert diluents (non-solubilizing cosolvents, such as TTE, or hydrogen fluoride ether (HFE)). The diluents reduce viscosity and improve wetting, but Li^+ remains primarily coordinated with solvents or anions incompatible with LiPS, forming 'high local salt concentration islands' (Figure 8c). Ren et al.[108] investigated the behavior of LHCE in battery applications based on four different types of model solvents, including DMC, tetramethylsulfonate, triethyl phosphate, and DME, to elucidate the intrinsic mechanisms underlying their differing behaviors in positive electrode materials. Cao et al.[110] systematically described the screening process for salts and solvents in LHCE in a review. Compared to traditional dilute electrolytes and HCE, LHCE has a unique solvation structure: high concentrations of salt-solvent clusters are distributed within non-solvated solvent (dilutant) molecules. Therefore, LHCE typically consists of three main components: ionic conductive salts, solvated solvents, and non-solvated diluents. The high solubility and dissociation constant requirements in HCE and LHCE exclude most lithium salts, such as lithium hexafluorophosphate ($LiPF_6$), lithium perchlorate ($LiClO_4$), and lithium tetrafluoroborate ($LiBF_4$). Salts based on imide anions, such as LiFSI, LiTFSI, and lithium bis(pentafluoroethanesulfonyl)imide (LiBETI), are the most suitable salts for HCE and LHCE.[110] Solemnization solvents offer more options. The basic requirements for such solvents in HCE and LHCE are similar to those in traditional electrolytes. Therefore, non-protonic solvents used in traditional electrolytes, such as DME,[119] EC,[120] DMC[121] and diethylene glycol dimethyl ether (G2)[122] are all good solvent candidates for HCE and LHCE. The purpose of the diluent is to reduce the total salt concentration in the final product while retaining the high salt-solvent clusters in HCE. The selection criteria for diluents are somewhat stringent. First, the diluent must have minimal or no solubility for the salt; second, the diluent must be easily miscible with the solvation solvents in HCE to prevent phase separation; third, the diluent must have weak solvation capacity for Li+ ions to preserve the local coordination environment of the solvation shell within HCE. Some excellent research has demonstrated that bis(2,2,2-trifluoroethyl) ether (BTFE),[121] 1,1,2,2-tetrafluoroethyl-2,2,3,3-tetrafluoropropyl ether (TTE),[123] or tris(2,2,2-trilfuoroethyl) orthoformate (TFEO)[124] are viable candidate diluents. However, most LHCEs use strongly solventized solvents to separate lithium salts, requiring high ratios of salt to solvent or diluent to solvent to achieve the desired anion-enriched solventized structure, which inevitably increases electrolyte costs.[110] The complexity of multi-solvent mixtures leads to unpredictable side reactions, and the relatively[122] high viscosity resulting in slow kinetics remains a challenge for researchers seeking to improve LHCEs.

3.3.3. Weakly Solvated Electrolytes

WSE, also known as low-solvent electrolytes, have solvation sheaths that contain solvents and anions that are coordinated to Li^+ ions through weak interactions, and can form anion-rich solvation structures to reduce the viscosity under dilution conditions (see Figure 7d). WSEs use solvents with lower dielectric constants, which inherently result in weaker solvation capabilities. Thanks to the unique solvation structure of WSEs, the formation of contact ion pairs (CIPs) and aggregates (AGGs) is promoted even at low to moderate salt concentrations. This unique characteristic stems from the weak interactions between salt ions and the solvent, leading to the preferential interaction of salt anions with Li+ and the formation of abundant CIPs and AGGs. As a result, the interfacial chemistry shifts from solvent-dominated to anion-dominated. Unlike HCEs and LHCEs, WSEs allow for the regulation of solvation structures at low concentrations, offering a potential solution to cost-related issues. Pham et al.[121] proposed a WSE for lithium metal batteries composed of 0.3 M LiFSI and 0.2M LiFSI with 1,4-dioxane (DX). In this electrolyte system, the primary salt anions, such as FSI^- and $TFSI^-$, exist in the form of CIPs and AGGs. Building on this, they designed a WSE for lithium-sulfur batteries composed of a mixture of 0.4 M LiTFSI with DX:dimethylmethanol (DMM).[122] Surface analysis confirmed the formation of a LiF-rich SEI layer, enabling uniform lithium deposition, with an average coulombic efficiency (CE) exceeding 99% after 100 cycles and an impressive initial specific capacity of 671 mAh $g^{-1}{}_S$. It was also noted that WSE can form an anion-derived SEI layer, thereby enhancing compatibility with lithium metal anodes and limiting the solubility of LiPS. Liu et al.[125] also demonstrated the role of WSE in promoting SEI formation. They developed a WSE based on a hydrophobic cyclopentyl methyl ether (CPME) solvent. It was demonstrated that due to the weak solvating properties and steric hindrance of CPME, the formation of a large number of contact ion pairs promoted the formation of an inorganic-rich SEI, thereby stabilizing the lithium metal. Li et al.[34] elucidated the mechanism underlying lithium anode corrosion and provided deeper insights into the interfacial kinetics. They demonstrated that reducing the electrolyte's LiPS solvation power—termed electrolyte solvation power (ESP)—effectively suppresses anode corrosion, albeit at the cost of retarded cathodic kinetics. With increasing content of weakly solvating solvents (WSS), ESP exhibits a two-stage trend, where the critical point depends on the penetration of WSS into the inner solvation shell of LiPS. Once WSS directly coordinates with LiPS, charge-transfer kinetics deteriorate sharply, leading to a rapid increase in activation polarization. However, existing literature on the effects of WSE on LSB is limited, suggesting that further research may be needed in this area.

3.4. Summary

The confinement of sulfur within the cathode matrix contributes to achieving a low E/S ratio by addressing key challenges at both electrodes. Selecting electrolytes with low solubility for elemental sulfur and lithium polysulfide (LiPS) species minimizes capacity degradation due to active material loss and mitigates lithium metal corrosion caused by soluble LiPS. Importantly, in cells operating via the solid-liquid-solid conversion mechanism, dissolution of LiPS increases the viscosity of the electrolyte, which typically would hinder Li^+ transport due to reduced ionic mobility. However, the presence of moderate concentrations of soluble LiPS can enhance ionic conductivity by increasing the total number of charge carriers (Li^+ and polysulfide anions), especially in dilute electrolytes. Nevertheless, when LiPS concentration becomes excessive, the resulting viscosity rise dominates, reducing bulk ionic conductivity and impeding electrolyte penetration into the porous cathode matrix. This reduced percolation restricts effective Li^+ transport to active sulfur sites, increasing overall cell resistance. Thus, suppressing soluble LiPS formation not only avoids parasitic reactions but also eliminates the need for excessive electrolyte to moderate LiPS concentration, thereby facilitating Li–S cells with a lower E/S ratio and more stable operation.

The approaches discussed here attempt to deal with the challenges associated with sulfur mobility by reducing the potential interaction of lithium polysulfides with the Li-metal electrode, in doing so, addressing not only the challenge of polysulfide shuttle but also removing the need to incorporate $LiNO_3$ as an additive, which offers significant promise in passing safety standards. By restricting the dissolution of lithium polysulfides these approaches also allow, in conception at least, the use of lower electrolyte volumes, which provides a broader design space for cells. Either offering the potential of ultra-high gravimetric energy density or reduced sulfur loadings for equivalent cell performance. The physically immobilized sulfur, either in confined pores or as a result of covalent attachment to a polymer backbone (i.e. SPAN etc.) do however, place an upper limit on the mass of sulfur in the composite electrode, with values of approaching 40–45% sulfur seen for SPAN as outlined previously. As a result, to achieve high energy densities in cells, the electrolyte volume must be low and sulfur utilization must be very high in both. Beyond these approaches, the use of electrolytes with low polysulfide solubility achieves similar effects while providing the ability to increase sulfur loadings in the positive electrode. This approach also necessitates reasonably low electrolyte volumes, though the higher sulfur loadings possible enable this to be somewhat larger than cells using physically immobilized sulfur. These cells are in a comparatively early stage of development when compared to the more conventional liquid electrolyte cells, which dissolve polysulfides during operation, though they offer promise to supersede the practical performance of these cells. For this to be realized an improved understanding of the mechanism of operation is required to develop a design framework for the positive electrode. Furthermore, the wider choice of electrolyte and salt combination may offer opportunities to explore alternative strategies in this space, with a particular focus on extending the stability of the negative electrode against Li-metal. Beyond electrode design, there are also significant research questions that must be answered relating to the degradation in this cell type. Identifying the critical interface and associated degradation modes will enable the development of strategies to extend lifetime in cells of high-energy density in these cells, which ultimately are likely to result in this format of cell exceeding the performance that is capable in a conventional liquid-based mechanism cell type.

4. Hybrid Quasi-Solid-State Electrolytes

4.1. Introduction

As discussed earlier, the main challenges, such as LiPS shuttle effect, lithium negative electrode instability and electrolyte consumption continue to hinder the development of battery with higher capacity and longer cycle life. To cope with these issues, researchers have proposed the use of solid-state electrolytes (SSEs) instead of liquid electrolytes. SSEs not only effectively avoid the safety concerns of flammable solvents but also inhibit the shuttle effect from the root cause due to the natural shielding of LiPS diffusion by its solid structure.[126] However, ASSLSBs face a series of engineering bottlenecks which poses a challenge to achieve high energy density and are at a very early technology readiness level (TRL) as discussed below in Section 5 (see Figure 2b).

In this context, QSSE Li-S cells have gained more attention as a synergistic integration point, combining the favorable electrochemical performance of conventional liquid-system batteries and enhanced safety of all-solid-state batteries, which also provides the opportunity to leverage the more mature technologies and manufacturing lines to facilitate a smoother path toward industrialization for lithium-sulfur batteries. QSSEs are generally composed of a polymer matrix (PQSSE) or an inorganic framework (IQSSE) with a small volume of liquid components introduced to form a gel-like or weakly gel-like composite system (**Figure 9**). This structure combines the ionic conduction efficiency of liquid electrolytes with the mechanical stability of solid electrolytes, effectively mitigating the poor contact at the solid-solid interface and significantly improving the overall safety and cycling stability of the system (Figure 9). The liquid-phase channels in the QSSEs offer continuous pathways for Li-ion transport, while the solid-phase matrix supresses the lateral LiPS diffusion and enhances the stability of the electrode-electrolyte interface.

Similar to the working mechanism of LELSBs, the sulfur contained in the positive electrode of Li-S cells with QSSEs undergoes a series of multi-electron reactions during the discharge process, which gradually reduces from S_8 to the soluble intermediates Li_2S_8, Li_2S_6, and further to the short-chained Li_2S_2 and the product Li_2S (see Figure 4). While in conventional LELSBs, the dissolved LiPS are prone to diffuse to the negative electrode, leading to the shuttle effect, the QSSE system is able to significantly inhibit the migration behavior of the polysulfide intermediates due to the physical constraints of the polymer/inorganic matrix and the optimal modulation of the electrolyte components (Figure 9). Upon systematic optimization, QSSEs can also safeguard the ion transport continuity, promoting the efficient conversion of LiPS, enhancing the sulfur utilization rate and prolonging the battery life. For example, Li et al.[127] developed a PQSSE electrolyte containing 13% free liquid by initiating the in situ ring-opening polymerization of DOL using metallic 1T-phase MoS_2 nanosheets. This PQSSE effectively regulated the dissolution-deposition pathway of LiPS by providing excellent

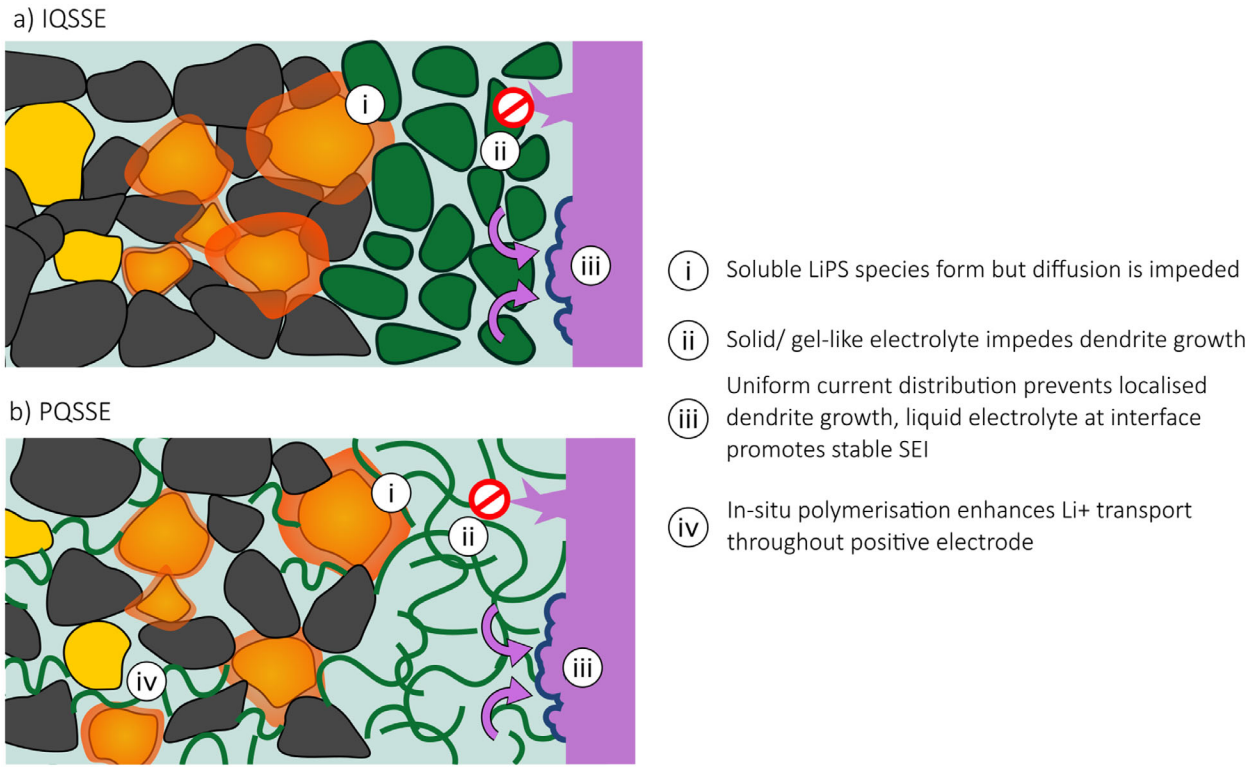

Figure 9. Sulfur to LiPS conversion mechanism in a) IQSSE and b) PQSSE. As in LELSBs, soluble LiPS species form, but the solid or gel-like components of the hybrid QSSE prevent diffusion. IQSSE after,[130,131] PQSSE after.[127,132,133]

interfacial wettability and superior ion channels and achieved a capacity retention rate of up to 80.7% after more than 200 cycles at an ultra-low electrolyte/sulfur ratio of 2 μL mg^{-1}, which demonstrated the great potential of quasi-solid state electrolytes in enhancing the long-cycle stability. Meanwhile, Das et al.[128] constructed a highly elastic PQSSE based on in situ polymerization of pentaerythritol tetraacrylate (PETEA). The PQSSE was able to maintain stable ionic conductivity and mechanical flexibility over a wide temperature range from −25 to 45 °C, and exhibited a capacity retention of 95% after 100 cycles at 2C rate, indicating that the quasi-solid system not only significantly inhibits polysulfide shuttling but also offers the potential for excellent high-rate performance and environmental adaptability.

As detailed, QSSEs are systems essentially composed of both solid and liquid QSSEs can be categorized into PQSSEs and IQSSEs, which are similar to SSEs, which are typically classified into solid-state polymer electrolytes and solid-state inorganic electrolytes.[129] These have been widely studied with a range of differing components and compositions of electrolyte. A selection of PQSSEs and IQSSEs reported in recent years with satisfactory electrochemical properties and high ionic conductivities is outlined in **Tables 2** and **3**.

4.2. Polymer-Based Quasi-Solid-State Electrolytes (PQSSE)

Polymer/inorganic hybrid quasi-solid-state electrolytes (PQSSEs) have emerged as a promising class of materials to bridge the gap between liquid and solid-state systems, combining the mechanical stability and safety advantages of solids with the ion transport flexibility of liquids. Recent research has shifted from simple gel electrolytes toward engineered composite systems that exhibit enhanced ionic conductivity, interfacial compatibility, and structural robustness tailored for lithium–sulfur (Li–S) batteries.

A major challenge in polymer-based QSSEs is their inherently low ionic conductivity, primarily due to the high crystallinity and limited segmental motion of common polymer matrices such as poly(ethylene oxide) (PEO). To overcome this, researchers have incorporated inorganic fillers like $Li_{10}SnP_2S_{12}$ (LSPS) into the PEO matrix to form composite electrolytes. These fillers disrupt the crystalline domains of PEO and provide fast ion-conducting pathways, enabling an ionic conductivity of 1.69×10^{-4} S cm^{-1} at 50 °C—significantly higher than that of pure PEO. Moreover, the uniform dispersion of LSPS improves the mechanical strength and interfacial stability with lithium, thereby enhancing Coulombic efficiency and cycling performance.[138]

Beyond conductivity enhancement, suppressing polysulfide shuttle and stabilizing the lithium interface remain key priorities. UV- or thermally initiated cross-linking strategies, such as those employing PETEA-based networks, have demonstrated the ability to form robust polymer matrices that suppress the diffusion of lithium polysulfides. However, such highly cross-linked structures often suffer from reduced ionic mobility and limited wetting at the electrode–electrolyte interface, indicating the need for precise control over cross-linking density.[125,128,139]

Poly(methyl methacrylate) (PMMA), another widely investigated matrix material, offers excellent chemical stability and processability. However, its mechanical fragility and poor ionic

Table 2. Composition and performance of recently reported PQSSEs.

Number	Positive Electrode	S loading	Solid state part	Liquid state part	σ/Scm^{-1}	Initial capacity/mAh $g^{-1}{}_S$	End of life capacity/ mAh $g^{-1}{}_S$ (cycle)	Highest C-rate	Reference
1	S:CNT:SP =7:1:2	0.5	PEO:PVDF: LiTFSI=7:3:2 in acetonitrile	15 μL of 1 M LiTFSI in DOL : DME (1 : 1) with 0.1wt% $LiNO_3$	N.A.	1810	1000 (150)	2C	[134]
2	S:C:PVDF:SP:CNT= 10:5:3:1:1	1.70	PETEA 5.3wt%+AIBN 0.3wt% in 0.7 M LiNO3+0.3 M LiTFSI in DOL : DME (1 : 1)	50 μL 0.7 M LiNO3+0.3 M LiTFSI in DOL : DME (1 : 1)	3.41*10^{-5}	919	472 (100)	2C	[128]
3	S@PPy:SP:PVDF=8:1:1	1.5	600 mg PVDF-HFP+300 mg PETT+100 mg PETEA+ 50mg SST in 3 mL DMF and 50 μL of 2-hydroxy-2-methylpropiophenone	1 M LiTFSI in DOL : DME (1 : 1) with 2wt.% $LiNO_3$	1.87*10^{-3}	N.A.	N.A.(150) 87.6% capacity retention	0.2C	[132]
4	N.A.	N.A.	ANF+Janus	N.A.	4.8*10^{-4}	1320.6	922.8 (100)	2C	[135]
5	(S:KB=7:3):Canrd=9:1	2.5-3.5	1 wt.% Tris(pentafluorophenyl)boron	2M LiTFSI in DOL	N.A.	1100	450 (150)	0.1C	[133]
6	(S:KB=3:1):(CNT:SP=2:1):La133=8:1:1	1.5	4mM $Al(OTf)_3$ in DOL	1 M LiTFSI in DOL : DME (1 : 1)	3.81*10^{-4}	908	625.7 (240)	1C	[136]
7	(S:CB=7:3):SP:PVDF=7:2:1	1.0-1.3	25wt.% PVDF in DMF with 1gL^{-1} PDA	1 M LiTFSI in DOL : DME (1 : 1)	N.A.	1215.4	868.8 (200)	2C	[137]
8	SPAN:SP:PVDF=7:2:1	2.5	(PVDF-HFP: LiTFSI=1:1) +20wt% SN in DMF	30 uL 1M $LiPF_6$ in EC:DEC=1:1	1.01*10^{-3}	1189	1118 (200)	10C	[138]
9	(PEI-GMA:S= 1:2):SP:PVDF=8:1:1		5mM PEI+5mM GMA in IPA	1 M LiTFSI in DOL : DME (1 : 1) with 2wt.% $LiNO_3$		734.9	668.7 (400)	2C	[139]

PETEA: Pentaerythritol tetraacrylate; AIBN: Azobisisobutyronitrile; PETT: Polymerization of pentaerythritol tetrakis (3-mercaptopropionate); PVDF-HFP: Poly (vinylidene fluoride-co-hexafluoropropylene); SST: soluble starch; SP: Super P; CNT: Carbon nanotubes; Py: Pyrrole; AC: Acid-treated carbon nanotubes; KB: Ketjen Black EPC-600JD; Canrd: LA133 binder; CB: Carbon black; PDA: Polydopamine; PEGDA: Poly-(ethylene glycol) diacrylate; PTFE: Polytetrafluoroethylene; G: Graphene; AB: Acetylene black; VGCF: Vapor grown carbon fibres; CN: Succinonitrile; EC: Ethylene carbonate; DEC: Diethyl carbonate; IPA: isopropyl alcohol; GMA: Glycidyl methacrylate; PEI: Polyethylenimine;

Table 3. Composition and performance of recently reported IQSSEs.

Number	Positive Electrode	S loading	Solid state part	Liquid state part	σ/Scm^{-1}	Initial capacity/mAh g^{-1}_S	End of life capacity/ mAh g^{-1}_S (cycle)	Highest C-rate	Reference
1	S-AC:SP:PVDF=8:1:1	2.5	PVDF+PMMA+LATP in DMF with 1 M LiTFSI in DOL : DME (1 : 1) with 2wt% $LiNO_3$	30 µL mg^{-1} 1 M LiTFSI in DOL : DME (1 : 1) with 0.2M $LiNO_3$	0.47	1184.8	802.7 (200)	5C	[127]
2	S:CNT:PVDF=64:26:10	2.0	LLZTO+PEGDA+AIBN	1 M LiTFSI in DOL : DME (1 : 1) with 1wt.% $LiNO_3$	$1.34*10^{-3}$	1201	656 (200)	2C	[134]
3	(G:S=1:1):AB:VGCF=7:1.5:1.5	N.A.	LLZO+PTFE	1 M LiTFSI in DOL : DME (1 : 1) with 2wt.% $LiNO_3$	0.7	1448.3	730.7 (40)	2C	[135]
4	S+CNF	3	LATP+ PIN	1 M LiTf-DME/DOL	0.1	950	800 (150)	0.5C	[140]
5	Li_2S:C=50:50	0.57-0.75	$Li_7P_3S_{11}$	$(MeCN)_2$-LiTFSI-TTE	N.A.	1287	1264 (80)	1C	[141]
6	S:CB:PVDF=70:20:10	1	LLCZN + Li–Al	1 M LiTFSI in DOL : DME (1 : 1)	4	1388	1000 (30)	N.A.	[142]
7	S:KB:SP:CNT:CMC:SBR=48:32:5:5:5:5	1.2-1.3	LAGP + AB:CNT:PVDF:6:2:2	LiTFSI-TEGDME	0.17	1409	1000 (50)	0.2C	[143]

AIBN: Azobisisobutyronitrile; PETT: Polymerization of pentaerythritol tetrakis (3-mercaptopropionate); PVDF-HFP: Poly (vinylidene fluoride-co-hexafluoropropylene); SST: soluble starch; SP: Super P; CNT: Carbon nanotubes; Py: Pyrrole; AC: Acid-treated carbon nanotubes; KB: Ketjen Black EPC-600JD; Canrd: LA133 binder; CB: Carbon black; PDA: Polydopamine; LLZTO: $Li_{6.5}La_3Zr_{1.5}Ta_{0.5}O_{12}$; PEGDA: Poly-(ethylene glycol) diacrylate; LLZO: $Li_{6.4}La_3Zr_{1.4}Ta_{0.6}O_{12}$; PTFE: Polytetrafluoroethylene; G: Graphene; AB: Acetylene black; VGCF: Vapor grown carbon fibres; CN: Succinonitrile; EC: Ethylene carbonate; DEC: Diethyl carbonate; IPA: isopropyl alcohol; GMA: Glycidyl methacrylate; PEI: Polyethylenimine; LATP: $Li_{1+x}Ti_{2-x}Al_x(PO_4)_3$ PIN: polymer with intrinsic nanoporosity; LLCZN: $Li_7La_{2.75}Ca_{0.25}Zr_{1.75}Nb_{0.25}O_{12}$; LAGP: $Li_{1.5}Al_{0.5}Ge_{1.5}(PO_4)_3$

conductivity limit its standalone application. Hybrid strategies, such as the in situ polymerization of methyl methacrylate in solvents like DME, have shown promise. Liu et al.[139] reported such an approach, yielding a gel electrolyte with superior C-rate capability and improved oxidation stability, owing to the formation of lithium-coordinated PMMA chains that facilitate selective ion transport.

Similarly, PVDF-based systems benefit from high dielectric constants and good interfacial adhesion to lithium, yet their strong polarity and moisture sensitivity hinder long-term cycling. Copolymerizing PVDF with hexafluoropropylene (PVDF-HFP) mitigates these issues by lowering crystallinity and increasing flexibility. However, PVDF-HFP alone still suffers from suboptimal ionic conductivity and potential structural defects during film casting.[127,130,141]

To address these multifaceted limitations, hybrid systems incorporating functional inorganic components have gained attention. For instance, Wang et al.[142] developed a PVDF-HFP/PAN blend reinforced with dopamine-coated LLZTO (PDA@LLZTO), a garnet-type ceramic. The resulting composite achieved a room-temperature ionic conductivity of 0.4×10^{-3} S cm^{-1} and maintained high capacity retention even at 0 °C. The PDA coating not only enhanced the filler–polymer interaction but also facilitated Li^+ transfer at the interface, thereby improving electrochemical stability and thermal endurance.

Taken together, these advances underscore a growing trend toward functionally integrated hybrid electrolytes, where each component is selected and engineered to address a specific bottleneck—whether it be ionic conductivity, mechanical strength, dendrite suppression, or interfacial stability. The synergy between polymers and inorganic fillers enables tailored microstructures and percolated ion transport networks, offering a viable route toward safer, high-energy QSSE-based Li–S batteries.

Further development in this field requires a mechanistic understanding of filler–matrix interactions, rational design of polymer architectures, and fine-tuning of ionic domains to simultaneously meet the demands of high conductivity, structural integrity, and interfacial compatibility (Figure 4). These strategies, borrowed from solid-state lithium-metal and lithium-ion systems, are now being adapted and optimized for the specific requirements of Li–S chemistry.

4.3. Inorganic-Based Quasi-Solid-State Electrolytes (IQSSE)

While polymer-based QSSEs offer enhanced flexibility and processability, their performance is often limited by insufficient ionic conductivity and interfacial stability. To further address these issues, inorganic-based quasi-solid-state electrolytes (IQSSEs) have emerged as a complementary approach, leveraging the superior mechanical and electrochemical stability of ceramic components.

Inorganic-based quasi-solid-state electrolytes (IQSSEs) integrate the high mechanical strength and ionic conductivity of inorganic solid electrolytes with the improved interfacial wettability of liquid phases, offering a promising pathway to address key challenges in lithium–sulfur (Li–S) batteries—namely safety, polysulfide shuttling, and lithium dendrite growth (Figure 4). By carefully incorporating a small amount of liquid electrolyte into a rigid inorganic framework, IQSSEs can simultaneously achieve high ionic conductivity, interfacial compliance, and stable long-term operation.

Among inorganic systems, sulfide-based solid electrolytes such as $Li_{10}GeP_2S_{12}$ (LGPS) and Li_6PS_5Cl (LPSCl) are known for their exceptionally high ionic conductivities (10^{-3}–10^{-2} S cm^{-1} at room temperature),[143] as well as their low interfacial resistance due to soft mechanical properties that conform well to lithium metal surfaces. However, their high sensitivity to moisture and air—leading to H_2S gas evolution—presents a significant barrier to practical application. To address this, Cao et al.[126] proposed a solvated salt complex, $[Li(triglyme)]^+[TFSI]^-$ (LiG3), that undergoes in situ electrochemical reduction to form a stable SEI on lithium and simultaneously stabilizes the LGPS matrix, demonstrating an effective interfacial engineering strategy for sulfide-based IQSSEs.

Oxide-based electrolytes, particularly garnet-type materials such as $Li_7La_3Zr_2O_{12}$ (LLZO) and its doped derivatives (e.g., Al^{3+}, Ta^{5+}), offer excellent chemical and electrochemical stability, non-flammability, and resistance to moisture. However, their rigid structure often leads to poor interfacial contact and high impedance with lithium metal. Hybrid approaches that combine oxides with flexible binders or absorbent structures have shown promise. AbdelHamid et al.[135] processed LLZO flakes into a porous yet cohesive framework using polytetrafluoroethylene (PTFE), enabling the uptake of liquid electrolyte and maintaining interfacial integrity without compromising mechanical strength — thus resolving both handling and interface wetting challenges.

Recently, halide-based solid electrolytes, such as Li_3InCl_6 and Li_3YCl_6, have gained attention due to their wide electrochemical stability windows (up to 4.5 V vs. Li^+/Li), favorable air/moisture stability, and lower interfacial reactivity with liquid components compared to sulfides.[144] These properties make them particularly well-suited for hybrid configurations where residual solvent or trace moisture may be present. Halide systems also demonstrate improved interfacial stability under mixed-phase conditions, thus emerging as strong candidates for the next generation of IQSSEs.[145]

Taken together, these examples reflect a progressive evolution in IQSSE material design, where sulfides emphasize high conductivity and compliance, oxides offer structural stability and chemical inertness, and halides strike a balance between electrochemical compatibility and interfacial robustness. This strategic tuning of electrolyte phases — often paired with targeted interfacial engineering — has enabled IQSSE-based Li–S batteries to achieve improved cycling stability, suppressed polysulfide diffusion, and enhanced safety under practical conditions.

Nevertheless, the interfacial complexity between inorganic phases and liquid/semiliquid additives remains a critical bottleneck. Future work must focus on understanding and tailoring interfacial reactions, particularly under high sulfur loading and dynamic volume change. Strategies such as interface-modifying coatings, flexible interlayers, and multifunctional inorganic frameworks may offer viable routes to stabilize these interfaces without sacrificing ionic transport or structural integrity.

4.4. Interfaces in QSSE Cells

In Li-S cells with QSSEs, the efficient migration of Li-ions and interfacial stability are the keys to achieving high energy density with long cycle life. However, due to their solid-liquid composite nature, QSSEs inevitably suffer from multiple interfacial problems, especially at the two key locations of the lithium negative electrode-electrolyte interface and the solid-liquid electrolyte interface, where the trade-off between interfacial contact, chemical stability, and the ability of continuous ion migration affects the battery performance.

4.4.1. Lithium Negative Electrode-Electrolyte Interface

One of the key roles of the Li/electrolyte interface is to stabilize Li by forming a high-quality SEI layer, thereby preventing the formation of Li dendrites and their side reactions with PS materials. Improving the quality of the SEI layer can be achieved using well-defined components from existing traditional liquid Li-S electrolytes. Zuo et al.[144] utilized $LiNO_3$ in the polymer network PQSSE to regulate interface stability by in situ forming a good SEI, thereby achieving uniform, dendrite-free Li deposition and highly reversible deposition/stripping processes. Similarly, for example, F^- and N^- based salts LiFSI, LiFTFSI and lithium azide (LiN_3), and nano-Al_2O_3 can effectively stabilize Li and enhance the quality of the SEI at the Li/electrolyte interface.[145–147]

PQSSE and IQSSE systems each have their own advantages and disadvantages in the contact area between the lithium metal anode and the electrolyte. PQSSE typically uses flexible polymer matrices such as PVDF-HFP or PEO as the main component, excelling at forming a physically tight and conformal interface with the lithium anode. This inherent flexibility maximizes the electrochemical active area, thereby minimizing initial contact resistance. However, this interface is far from static. The primary driver of resistance growth in PQSSE is the continuous decomposition of liquid electrolyte components within the gel. During non-uniform lithium stripping and deposition processes, fresh, highly active lithium surfaces are repeatedly exposed. This triggers ongoing parasitic reactions, leading to the gradual thickening of the SEI. Although the initial SEI may exhibit ionic conductivity, its continuous and typically non-uniform growth increases bending and ionic transport resistance during cycling. This leads to a gradual increase in battery polarization and a decrease in coulombic efficiency. The fundamental weakness of PQSSE lies in its low mechanical modulus. While they can accommodate minor volume changes, they cannot provide sufficient mechanical resistance to prevent lithium dendrite growth, especially at practical current densities. This mechanical flexibility leads to the formation of filamentary lithium, which slowly penetrates into the electrolyte, causing a 'soft short circuit'.[148] While applied stack pressure helps maintain contact, it is largely ineffective in preventing dendrite growth in this soft medium, as the pressure required to mechanically block lithium far exceeds what the polymer structure can withstand without deformation or failure.

IQSSE-based cells typically employ rigid ceramic supports, such as Li_6PS_5Cl or $Li_7La_3Zr_2O_{12}$, which, according to the Monroe-Newman 'dendrite' model,[149] have sufficiently high mechanical modulus to effectively inhibit the growth of lithium dendrites. However, these cell's performance is severely limited by poor interfacial mechanics and dynamic resistance growth. The rigid, non-deformable nature of ceramics results in poor point-to-point physical contact with the lithium anode, leading to high initial interface resistance. Additionally, during lithium stripping, voids inevitably form at the interface.[150] Unlike liquids or gels, rigid ceramics cannot flow to fill these voids. This results in a sharp decrease in the electrochemically active area and a corresponding surge in contact resistance, which typically dominates the battery's overall impedance. During cycling, high stress concentrates on a few actual contact points, potentially causing brittle ceramic fracture. Lithium grows through these newly formed microcracks, offsetting the advantage of high modulus. Additionally, many IQSSEs are thermodynamically unstable with lithium, leading to the formation of mixed conductive interface phases, which cause a continuous increase in interface resistance.[151] These phenomena are further discussed later when outlining the potential of all-solid-state Li-S batteries.

During battery manufacturing and operation, applying pressures of several hundred MPa is a simple, but practically ineffective, method to enhance lithium/electrolyte contact.[152,153] In all cases discussed in this work, high pressures have been applied to the cell, highlighting both the comparatively nascent stage of this research field and the need to consider the practical limitations that will be employed on a technology when in the field as this technology matures. In Lin et al.'s[154] study, Li_3PS_4 was directly cold-pressed onto a 50 µm thick lithium foil under an external pressure of 240 MPa to achieve a structurally dense and fast ion-conducting effect. The Li-S batteries exhibited good rate performance from 0.1 to 2C at 60 °C. Introducing a buffer layer between the lithium metal and electrolyte is another method to enhance interface contact. Hakari et al.[155] placed a 300 µm thick indium foil and a 250 µm thick lithium foil on the SSE surface, then compressed them into an integrated block under 72 MPa pressure. Compared to pure lithium, the indium buffer layer exhibits a higher Li^+ ion diffusion rate, which facilitates ion transport to the interface and enables uniform lithium deposition.

It should be noted that while applying external pressure is necessary to achieve optimal battery performance, the low yield strength of lithium may cause it to extrude through microcracks in the QSSE, leading to mechanically induced short circuits. Therefore, a structurally dense QSSE is crucial for preventing the formation of lithium dendrites. Additionally, the volume changes and resulting internal stresses accompanying continuous charge–discharge cycles in lithium anodes during cycling cannot be ignored. These changes induce the growth of lithium dendrites that envelop electrolyte particles, ultimately leading to interface failure between the anode and electrolyte.[156] Therefore, when considering the lithium/electrolyte interface in QSSE, it is essential to comprehensively account for the mechanical properties of the electrolyte, pressure, and interface reactions and changes during long-term cycling.

4.4.2. Solid–Liquid Electrolyte Interface

The second critical interface in the QSSE system is the contact region between the solid state and the liquid electrolytes. This interface directly affects the transport continuity of Li-ions and

the migration path of intermediates (e.g., lithium polysulfide). In conventional ether electrolytes, Li-ions are solvated by solvent molecules and then migrate; in inorganic-based electrolytes, Li-ions are conducted as hopping; and in polymers, Li-ions are conducted by solvation and desolvation as the polymer chain segments move.[157]

Therefore, the mechanisms involved in analyzing Li-ion conduction in quasi-solid electrolytes are very complex. In polymer quasi-solid systems, liquid components (e.g., DOL:DME) are adsorbed or encapsulated in the polymer network to form a gel-like structure, and their good compatibility usually leads to low interfacial impedance and high ion migration efficiency. However, the solvent may cause structural collapse due to volatilization or segregation at high temperatures or long cycling times, leading to degradation of the cell performance.

For inorganic QSSE systems, the liquid electrolyte mainly exists as an interfacial wetting agent to assist in improving the ion contact and transport between inorganic particles or between them and the electrodes, but the stability of such solid-liquid interfaces is poor. Liquid components are prone to induce side reactions at the interface, including decomposition in contact with Li_6LiPS_5Cl or side reactions with metals, leading to electrochemical instability at the interface and generation of undesirable by-products (e.g., Li_2S or Li_3PO_4, etc.).[158] This not only blocks the ion channels but also may cause problems such as interface polarization and impaired cycle life. For this reason, researchers have proposed the use of pre-coated wettable polymers, the construction of artificial interfacial layers, or the development of more compatible sulfide/oxide composite electrolytes to improve the chemical stability and structural integrity of the solid–liquid junction.[159]

Therefore, the optimization of the two interfaces in Li-S cells with QSSEs needs to be considered separately for the intrinsic properties of different QSSE systems. The polymer system focuses more on enhancing interfacial wettability and flexibility to reduce impedance, while the inorganic system needs to improve interfacial mechanical integrity and chemical compatibility to enhance cycling stability. The future direction of development may be to complement the advantages of the two types of materials to build multilayer synergistic structures, such as the interface engineering strategy of 'polymer-coated inorganic electrolyte', to achieve the unity of high conductivity and high stability.

4.5. Summary

Li-S cells with QSSEs present a promising compromise, integrating the high ionic conductivity of liquid electrolytes with the enhanced safety and stability of solid-state systems. These hybrid systems, typically composed of a polymer or inorganic matrix containing a small amount of liquid electrolyte, effectively mitigate the polysulfide shuttle effect while maintaining relatively good interfacial contact. In addition, QSSLSBs can achieve stable cycling and high capacity retention, even under practical conditions such as low E/S ratios. It should be noted, however that some polymers do show polysulfide solubility, which may result in isolation of active material in the electrolyte, limiting lifetime.

Despite these advantages, the development of Li-S cells with QSSEs faces significant challenges rooted in their composite nature due to the 'solid and liquid' hybrid system. For example, interface contact issues originating from solid components, lithium polysulphide shuttling effects originating and short lifespan from liquid components, have only been alleviated but not completely resolved. Therefore, it is unwise to consider only the solid or liquid phase when developing this type of QSSEs. Ultimately the performance of this cell type will be governed by the ability to design a sufficiently mechanically robust hybrid electrolyte which displays sufficient ionic conductivity. This challenge is similar to that faced by all-solid-state cells, though the comparative flexibility of these hybrid electrolytes likely makes overcoming mechanical challenges more straightforward. Practically, this is likely to be the most substantiation challenge that must be overcome to enable this cell format to be deployed in the field. Once again, this cell format is in a comparatively early stage of development compared to conventional liquid-based electrolyte cells, which results in significant questions regarding the operating mechanism and degradation modes of these cells, which are likely to occur both at the positive and negative electrode interfaces with the electrolyte. These interfaces are comparably stagnant when compared to the liquid-based systems discussed previously, which necessitates overcoming challenges regarding passivation and reactivity of the electrodes with the electrolyte either directly or via dissolution mechanisms.

5. All-Solid-State Lithium-Sulfur Batteries

5.1. Introduction

The solid-state battery has long been considered a route to extending energy density in Li-ion systems, allowing the use of a Li-metal electrode. When considered in a Li-S format the potential benefits shift somewhat; whilst also hypothetically providing the most promising energy densities for the sulfur chemistry, this cell format significantly reduces the dynamism of the interaction between the Li-metal electrode and the electrolyte when compared to a liquid electrolyte cell by both stabilizing the interface and eliminating routes for the shuttle reaction offering the prospect of significantly extended lifetimes.[160] Crucially, this cell format also removes the need to use $LiNO_3$ within the cell. As with the Li-ion solid-state cells, there remain significant barriers to the commercialization of this cell format, including the production of solid-state electrodes with sufficient ionic conductivity, the scaling up and manufacture of these components in a sufficiently thin format and interfacial resistances.[161–163] However, when considering an ASSLSB, the additional challenges posed by an electronically insulating active material, which undergoes a conversion mechanism rather than the more conventional intercalation materials used in Li-ion systems, are substantial. In particular, the volume expansion which occurs upon conversion of S_8 to Li_2S of 80% in a solid-state format is likely to result in rapid pulverization of the positive electrode without significant efforts being made to accommodate this change within the architecture of the battery. Despite the greater challenges in deploying a sulfur-based positive electrode, the benefits compared to a traditional mixed metal oxide are significant due to sulfur's outstanding theoretical electrochemical capacity of ca. 1675 mAh $g^{-1}{}_S$ (vs <300 mAh g^{-1} in NMC-based materials). The promise of this cell type, therefore is attracting increasing interest with work

ranging from developing an understanding of the fundamental reaction mechanism within ASSLSBs, which is necessarily different due to the lack of liquid electrolyte required to form intermediate LiPS.

5.2. Mechanism

The overall electrochemical reaction for a SSLS cell is the same as a conventional liquid cell, with a product of Li_2S/Li_2S_2 formed from the reduction of elemental sulfur, S_8. However, in sharp contrast to the reaction schemes discussed in Sections 2–4, in an ASSLSB the characteristic double plateau does not appear during discharge of the solid-state counterpart (see Figure 4g). This plateau, as detailed in Section 2.2, is attributed to the formation of a range of intermediate LiPS of varying solubility in the liquid electrolyte. In a solid-state format, this mechanism is not available, with the monotonic discharge curve observed in this cell format has historically been discussed as evidence for a direct S_8 to Li_2S reaction occurring during discharge.[69,164–167] This hypothesis has, in more recent times, been questioned by Cao et al.[168] identifying the presence of Li_2S_2 as an intermediate polysulfide during discharge using a combination of Raman spectroscopy and ex situ X-ray absorption spectroscopy (XAS). The authors highlight that this polysulfide is not soluble in conventional liquid electrolytes; therefore, its formation is not impeded by solvation issues, which preclude the production of higher order LiPS in ASSLS cells. They also note that the formation of Li_2S_2 contributes half of the theoretical capacity of the cell (ca. 1675 mAh g^{-1}_S) and in their experimental work the discharge capacity achieved of 1200 mAh g^{-1}_S suggests that the kinetic limitations imposed by the formation of Li_2S_2 in the cell and subsequent conversion to Li_2S are likely to be performance limiting steps within this discharge mechanism, with a mixed Li_2S_2/Li_2S discharge product produced. This mixed product, while not maximizing the electrochemical performance of the system, has been shown to improve the cycle life and stability of ASSLS cells with challenges in achieving reversible conversion of Li_2S to S_8 discussed by Kim et al.[169] Here, the authors delivered 1500 cycles by limiting the lower discharge of the cell to 0.6 V. The authors assigned this high cyclability to the improved electrochemical cycling of Li_2S_2 compared to Li_2S and a reduced volumetric expansion, which limits the pulverization of the electrode. This multistep conversion mechanism is in keeping with the thermodynamic favorability of polysulfide formation, which has been reported in liquid phase systems by Wang et al.[170] Indeed, the vast majority of ASSLB reports do not show full electrochemical conversion of S_8 with typical capacities ranging from 1100–1400 mAh g^{-1}_S. This incomplete sulfur conversion suggests that the dominant mechanism in an ASSLS battery promotes a mixed product of Li_2S and Li_2S_2. Recent work in a liquid phase system has proposed a mechanism for sulfur reduction, which includes the solid-state electrochemical reduction of Li_2S_2 to form Li_2S.[38] This proposed model differs from that proposed by Lu et al[171] and others who have suggested that the Li_2S_2 to Li_2S occurs via a disproportionation reaction which is independent of the potential observed during the reaction. It should be noted that these studies are in liquid based cells; however, the lack of direct consensus highlights the complexity of the system, which has been studied in much more detail than the ASSLS equivalent. Alongside these works in the liquid system, Yang et al.[172] have observed the direct conversion of S to Li_2S using a range of techniques, including in situ TEM and electrochemical energy loss spectroscopy (EELS). This work concluded that the lithiation of sulfur occurred first via phase separation of the initial sulfur particle, with the formation of nanocrystals of Li_2S and sulfur occurring before the remaining sulfur is converted to Li_2S. Whilst the authors in this work did not identify the presence of Li_2S_2 the lack of the higher-order LiPS suggest that while the mechanism for solid-state conversion is not currently well defined the presence of high order LiPS in the reaction is unlikely. The solid-state conversion of sulfur has been discussed in detail by Kim et al.[148] who argue that the complexity of the conversion mechanism requires substantially more investigation than has been previously assumed. In particular, the authors note that the kinetic limitations in an ASSLS positive electrode are significantly higher than in a conventional cell as the sulfur species do not dissolve and move away from the initial sulfur particles. Given the considerable uncertainty that remains in the solid-state conversion mechanism it is clear that further research is needed to identify the specifics of the reaction scheme alongside rate-limiting steps. In particular research should target the identification of rate-limiting steps and the mechanisms by which the conversions occur to enable the targeting of appropriate catalysts (be they conventional or electrocatalysts). An improved understanding of this route would also allow the tailoring of the mixed discharge products to maximize the durability of a practical system. While a fundamental understanding of the complete mechanism is an outstanding challenge across all formats of the Li-S cell, it should be noted that the mechanisms in an ASSLS battery would be expected to be more facile and controllable than that observed in a liquid electrolyte.

5.3. Material Selection

5.3.1. Solid State Electrolyte

All solid-state battery configurations are amongst the most widely researched in the literature, in particular for Li-ion chemistries, with frequent reports demonstrating promising progress in specific areas of the cell type. However, due to the complexity in manufacturing full cells, these results are often reported with unrealistic cell parameters, including elevated pressures, high electrolyte and negative electrode excesses and low sulfur loadings in the positive electrode. Whilst much can be learned from these targeted experiments, and the relatively early TRL of ASSLSBs (Figure 2b) necessitates fundamental development, it is also important to consider the requirements for the cell format which will enable cell gravimetric energy densities of 500 Wh kg^{-1} or greater. Benchmarking activity undertaken by Randau et al.[173] highlighted these challenges, showcasing a range of reports in which electrolyte thicknesses in the order of several 100s of microns were used for a range of solid-state configurations, including ASSLS cells. To achieve a practical cell, however this thickness will need to be significantly reduced to approaching 50 µm, with common recommendations being ca. 30 µm,[174] although this will naturally change when considering different material classes of electrolytes. The rationale for this is two-fold: firstly,

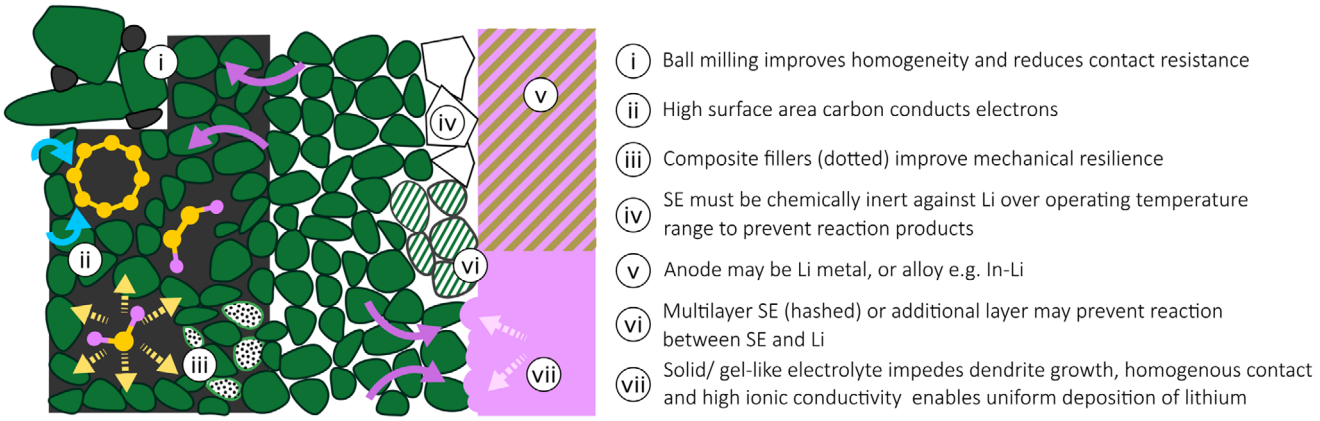

Figure 10. Schematic overview of key features and challenges of ASSLSBs.

the ionic conductivity of most materials necessitates thin electrolytes to avoid excessive Ohmic polarization during operation. In addition, the electrolytes which have been commonly explored are often very dense in comparison to liquid alternatives, resulting in a significant mass contribution to the cell of up to 60% in contrast to the 40–50% seen in liquid-based systems.[20,160,175] Alongside this requirement for thin processing in a practical cell, the materials used must be electrochemically, chemically and mechanically stable during operation, allowing for sustained operation. In common with transition metal oxide-based solid-state batteries, the porosity of the solid electrolyte is a crucial factor in ensuring the operability and durability of ASSLSB. Highly dense electrolytes are favored due to the more uniform Li concentration and reduced likelihood of dendrite formation[176,177] during operation, which results in improved negative electrode-electrolyte stability and avoids the fracturing of the electrolyte.[178] This further allows for the formation of a stable Li rich SEI, which is known to be related to the current density of operation,[179] and can minimize the resistance and degradation at the negative electrode. However, it is undoubtedly the positive electrode interface that poses the greatest challenges for ASSLSBs. Here, the volume expansion of the positive electrode results in a highly dynamic interface (**Figure 10**vii), which when coupled with the variable electronic and ionic conductivity provided by sulfur composite positive electrodes, result in non-ideal conversion efficiency and mechanical disconnection of the electrode from the electrolyte.[180]

The selection of the electrolyte in an ASSLSB is one of the most important choices that will determine the cell's performance, with this component requiring chemical and mechanical stability against two complex interfaces during operation. The manufacture of these components has been reported using a range of materials which can broadly be considered as inorganic (including halide, sulfide or oxide) or polymer-based as highlighted previously. These two classes of electrolytes can also be combined to form a hybrid or composite electrolyte that may be further supplemented with additional components as detailed in the discussion of QSSLSBs previously. Irrespective of the choice of material, the critical factors which should be considered include electrochemical stability, ionic conductivity, manufacturability (including the potential to produce thin films and air sensitivity) alongside the cost of any solution. While research has been conducted on a wide range of materials, the practical requirements which will be imposed on the component will constrain the choice of material in a real cell. This was highlighted by Yang et al.[181] who discussed the impact of the material choice on the gravimetric energy density of a theoretical ASSLS cell. In this work, they demonstrated that the typical density of oxide materials requires exceptionally thin electrolytes to deliver a cell with a high gravimetric energy density. This was expanded upon by Brown and Pasta[160] who highlighted this challenge by comparing the solid electrolyte volume to capacity against the solid electrolyte thickness for a wide range of materials and established a critical metric of <5 μL mA h^{-1} for practical use in a cell. This analysis reinforces the view that halides,[182] sulfides[183] and polymers[184] are the only materials that are likely to be deployed in a practical cell where energy density is targeted due to the very high density of oxide materials.[185] Each of these classes of materials also adheres to the requirement for reasonable processibility and is stable within the electrochemical window likely to be observed in an ASSLS cell (see Figure 4g); however, the materials have different ionic conductivities, stabilities and mechanical properties, which is likely to guide future design. Polymers for instance, typically show ionic conductivities in the order of 10^{-5} S cm^{-1} in contrast to the upper limit of 10^{-2} S cm^{-1} for sulfides and 10^{-3} S cm^{-1} for halides. Furthermore, sulfides and halides are sensitive to water, requiring processing in a dry environment. These are however, generally more mechanically robust than polymers, which impacts electrolyte and cell manufacture and the final cell's resistance to electrolyte fracture.

In addition to the reduced mechanical strength of polymers, research has shown that the PEO-based materials, which contain a mixture of Li containing anions and a PEO backbone and are amongst the most commonly discussed polymers for this purpose, can allow the formation of dissolved polysulfide species, which can further result in the occurrence of polysulfide shuttle even in an all-solid-state configuration.[186] Whilst the rate and extent of shuttle is not as severe as that observed in a liquid cell, it is undoubtedly a severe drawback for SSLS batteries and must be overcome should this material be deployed in the field. To overcome this a range of strategies have been suggested, including using materials which contain dual anion capability,[187] multiple polymers.[188,189] In general, the use of polymers has been most

widely observed in hybrid electrolytes (such as those discussed previously) as a result of the improved ionic conductivity provided by additional Li-ion conducting materials deployed.

The most commonly observed class of material used in solid-state electrolytes for ASSLSBs is the sulfides. These materials offer very high ionic conductivity at reasonable temperatures and are sufficiently processible to ensure the formation of good interfaces during cell manufacture without the need for high temperature sintering, which is not feasible in a Li-S cell.[190] Despite this promise, the materials are highly sensitive to water, evolving H_2S when exposed, and therefore require very dry environments for handling and processing.[45] Within this class of materials, the lithium argyrodite (Li_6PS_5X, X = Cl, Br, I) and LGPS ($Li_{10}GeP_2S_{12}$) are perhaps the most promising and have attracted the widest interest. The research in this area has tended to focus on substitutants and dopants to improve the ionic conductivity and stability of these electrolytes. Unlike polymers, these materials often interact negatively with polar solvents, with a consequent loss of ionic conductivity and therefore are not easily castable into thin films using these solvents.[191] To overcome this, several research efforts have explored the use of non-polar solvents and ionic liquids to accommodate tape casting and standard manufacturing routes.[192,193] Furthermore, the use of composite electrolytes using these materials with rubber has been shown to allow for the production of thin electrolytes[194] using routes which are similar to those observed via dry processing routes, which are emerging as an industry standard for Li-ion electrodes and may find use in this area.[50,51]

The use of halides compounds which contain lithium at least one metal and at least one halogen element in the general structure $Li_{3+m}Me_{1+n}X_6$ has emerged in recent years and offers significant promise as shown in a number of studies.[195–197] Whilst the elevated electrochemical stability of these materials has guided the focus of these materials toward Li-ion type chemistries there is undoubtedly some promise in their use in SSLS batteries. At present, these materials often use scarce and expensive components as a result, research is focused on developing more economic alternatives[190] alongside improving the ionic conductivity of these materials.[198]

5.3.2. Positive Electrode Design

Alongside the importance of selecting an appropriate solid-state electrolyte, the design of the positive electrode is crucial to maximize the gravimetric energy density and rate performance of an ASSLS cell. The interface between the negative electrode and the electrolyte in the ASSLSB format provides several of the same challenges as those observed in a solid-state Li-ion cell; however, the reduced potential of operation of the Li-S cell compared to its Li-ion counterpart reduces the likelihood of solid-electrolyte oxidation during cycling. In keeping with conventional LELSB systems, the highly insulating nature of sulfur necessitates the use of conductive additives in comparatively high quantities to enable the reduction of elemental sulfur to occur. However, as discussed in the case of ASSLSB, this reduction does not occur via the formation of intermediate polysulfide species, which exposes unreacted elemental sulfur to the ionically conductive electrolyte, allowing for the continued reduction of sulfur (Figure 4h). The immobilized nature of sulfur in an ASSLSB electrode necessitates the inclusion of ionically conductive pathways throughout the electrode. This additional design requirement essentially introduces a fixed triple phase boundary challenge which must be optimized to provide sufficient ionic and electronic conductivity through the electrolyte while ensuring a sufficient sulfur loading (and distribution) to achieve the conversion efficiency and capacity required to deliver high gravimetric energy densities (Figure 10 ii). This has generally seen positive electrodes developed with lower sulfur loadings than would be observed in LELSBs.[160] This design strategy has also seen efforts made to minimize the size of the sulfur particles used to maximize the surface area of the reactant and increase the likely triple phase boundary density. Alongside this initial design consideration, the conversion of sulfur to Li_2S or a mixture of Li_2S_2/Li_2S necessitates the accommodation of substantial volume changes during operation, which can in turn lead to pulverization of the electrode. To overcome this a polymeric binder is generally employed to maintain the structure of the electrode; however, this expansion can also be controlled by imposing lower voltage limits, sacrificing capacity at low potential to moderate the microstructural changes observed in the electrolyte.[169]

In keeping with many liquid-based positive electrodes, ASSLS cells are often produced using a composite sulfur containing material (often a S/C composite), which is then mixed, typically via ball milling, with a different carbon and ionic conductor (typically the electrolyte used) to increase the electronic and ionic conductivity through the electrode[174] (Figure 10i). This composition of electrode allows for acceptable kinetic performance, with the rate-limiting factors being reported as a combination of ionic conductivity and diffusion within the sulfur-containing species.[199] The first example of this described in detail was reported by Hayashi et al.[200] who used a S/Cu composite material mixed with acetylene black and a Li_2S-P_2S_5 ceramic and achieved a capacity of *ca.* 440 mAh $g^{-1}{}_S$ a capacity that was replicated by Agostini et al using a S/graphite composite.[201] Since then, significant developments in ionic conductors and improved electrode manufacturing have allowed for improved capacity and rate performances to be demonstrated. Ohno *et al.*[202] achieved over 1000 mAh $g^{-1}{}_S$ using a ball-milled sulfur/C65 composite, which starkly contrasted with a similar electrode manufactured by hand-grinding, which delivered only 220 mAh $g^{-1}{}_S$. This work clearly highlights the importance of ensuring an adequate extent of mixing in the production of a composite material and the conductive components in an ASSLS electrode. A similar capacity was reported by Chen & Adams[203] who used a S/Super P/Li_6PS_5Br composite to increase the capacity retention of the cell, showing relatively stable operation for up to 50 cycles.

A secondary method of manufacturing the positive electrode focuses on dissolving sulfur in a solvent and depositing it on the surface of an electronically conductive component, as described by Zhang et al.[204] While this process has been shown to produce reasonable capacities, exceeding 1200 mAh $g^{-1}{}_S$, the sulfur loadings achieved are significantly lower than would be required in a practical cell, in this work being reported as 0.5 mg cm^{-2}. Other efforts have focused on the use of sulfur-containing

conversion materials, including FeS_2[205,206] and MoS_2[207] however the performance derived from these electrodes has not matured to a level at which they could be considered for practical deployment in cells.

In more recent times, capacities exceeding 1000 mAh g^{-1}_S have become increasingly common in electrodes with higher sulfur loadings. Wang et al. have demonstrated over 1100 mAh g^{-1}_S in an electrode with 60% sulfur loading with a lifetime exceeding 600 cycles using a S/Ketjen black composite and Li_3PS_4-$2LiBH_4$ electrolyte.[208] The authors ascribed this strong performance to the low primary particle size and density of the solid electrolyte used, which allows improved uniformity in the positive electrode (Figure 10i), reducing the risk of the formation of large sulfur particles upon cycling. Chen et al. attempted to understand the challenges associated with the lifetime of SSLS cells, demonstrating over 1200 mAh g^{-1}_S in the first cycle.[209] Here the authors noted that contact losses between the electrode and electrolyte are most commonly observed during charging of the cell. To overcome this, indium was incorporated into a S/Ketjen black/LPSC composite, which provided a large increase in cyclability, allowing ca. 700 cycles to be achieved with 80% capacity retention and ca. 50% capacity retention after 1300 cycles. Capacity recovery was also observed when the cell was re-pressed, suggesting that a proportion of the degradation of the electrode could be ascribed to the separation of the triple phase boundaries within the electrode.

Efforts to improve the practical relevance of ASSLSB in recent times have seen an increased focus on achieving a credible active material loading and improved rate performance of the system. Nagata et al. produced an electrode with a loading of nearly 5 mg $cm^{-2}_{S,}$ achieving high capacity retention >90% after 100 cycles.[210] In the work, the authors also demonstrated a capability to achieve 1000 mAh g^{-1}_S at a rate of 3.2C which points to the promise of this approach. Song et al.[211] more recently demonstrated fast solid-sulfur reduction was demonstrated using a LBPSI glass-phase solid electrolyte with a comparatively low sulfur loading of 1 mg cm^{-2}. The work showcased high conversion efficiency of over 89% at a 2C charging rate with a capacity of just over 1400 mAh g^{-1}_S demonstrated. This work also showed outstanding cyclability with 1,375 mAh g^{-1}_S retained after 500 cycles. In this case the authors reported that the oxidation of Li_2S is mediated by the LBPSI which improves the conversion efficiency of the system. To enable this, work the authors first produced a sulfur/Ketjen Black composite before ball milling this composite with Super P carbon and the ionically conductive materials resulting in a sulfur content of 30%.

The significant development in the field from early electrodes, which provided ca. 25% of the theoretical capacity, to the high-rate, durable electrodes that have been reported highlights the potential of ASSLS electrodes. In general, the design of solid-state positive electrodes has been reported in conjunction with developments in the electrolyte, suggesting that there are significant gains to be made by a concerted effort to develop and design optimized architectures based on a single baseline solid-state electrolyte. Indeed, it is likely that 3D image analysis coupled with multiscale modelling may provide a useful tool to determine the most desired microstructure and provide design frameworks for future developments.[212–214]

5.3.3. Negative Electrodes

To maximize the gravimetric energy density of ASSLS cells, a low excess Li-metal electrode is preferred; however, this has been widely observed to come at the expense of a practical lifetime. Generally, the mass penalty for increasing the Li reservoir is relatively small, therefore it would be expected that even in a practical cell, a significant Li excess would be observed. This expectation has been reflected in the majority of the research discussed previously, in which large Li excesses have been used to remove performance limitations from the negative electrode in studies.

The challenges associated with plating metallic Li are well understood in the literature, with these particularly prevalent in solid-state systems,[215,216] in which intimate contact between the negative electrode and electrolyte is more challenging to maintain than in a liquid system. Alongside this, there is a need to form a stable SEI between the negative electrode and electrolyte in the cell and ensure planar plating of Li.[161] Approaches to resolve this, which have been applied in conventional solid-state cells, including the use of interlayers that mediate the mossy growth of Li by forming an alloy with the plated Li.[217,218] This approach has shown huge promise[219] although the cells can suffer from volumetric expansion associated with the alloying process which can lead to degradation at the negative electrode.[220] More broadly the use of alloyed negative electrodes (Figure 10v), in which Li is introduced to the system as an alloy of a range of metals has also shown promise, with improved plating and stability observed across a range of systems.[221] The volume expansion (and reversibly contraction) of these alloys (Figure 10vii), and Li-metal electrodes in general do however pose a challenge in maintaining stack pressure, which is common to all solid-state cells.[222] This is particularly pressing in mass sensitive applications where the additional componentry required to achieve appropriate stack pressures is likely to add significant parasitic weight to a practical cell. In the majority of studies which have reported ASSLSB performance the stack pressure is significantly often more than 50× the reported commercial target of 1–2 MPa.[223] In recent times the focus of more common transition metal oxide solid-state cells has shifted toward their high volumetric energy density,[224] driven largely by the automotive sector, but this is a factor which must be overcome to allow the deployment of an ASSLS cell which will more likely target different applications.[225]

There have also been efforts to investigate the potential of zero excess Li systems, although these have tended to be focused on liquid systems due to their complexity. This approach may offer valuable benefits in manufacturing ASSLSB due to the removal of the need to handle and/or deposit metallic Li. In these systems, the positive electrode is generally comprised of the discharge product, Li_2S, which is oxidized during the first cycle to produce an ASSLS cell. These systems tend to suffer from a poor first cycle efficiency, which result in an accessible Li deficit in the cells and consequently demonstrate poor capacity and lifetime. This approach in a LELSB cell was reported by Nanda *et al.*[226] who demonstrated the potential of this approach with 51% of the initial capacity retained after 100 cycles, with a large proportion of this lost in the first cycle when Li is seeded on the copper current-collecting foil. The activation and charging of Li_2S has also been highlighted as a route to capacity losses in these zero

excess systems[227,228] while Cruddos et al.[229] studied the impact of using different foils as current collectors in a zero-excess Li-S system. This study highlighted the benefit to capacity retention of moving beyond copper as a substrate, though it should be noted that the mass and processability of any foil must be considered for cells targeting high gravimetric energy density. This study also detailed the changes in the positive electrode morphology using X-ray computed tomography (XCT), once again highlighting the challenges in achieving an acceptable first cycle efficiency. To overcome this significant challenge, researchers have explored a range of catalytic and electrocatalytic approaches,[230,231] design strategies for the positive electrode[232,233] and negative electrode substrate modifications,[234,235] which may benefit future deployment in a solid-state cell.

While these approaches have all yielded benefits in liquid systems, alongside a significant number of studies focused on altering the liquid electrolyte, which are not relevant for ASSLS cells, there is a pressing need to improve the mechanistic understanding of the sulfur redox in solid-state cells. By gaining a firm understanding of the reaction pathways associated with charge and discharge, it will be possible to tailor approaches to target rate and performance-limiting steps, unlocking the potential of this chemistry.

5.4. Conclusion

Whilst ASSLSB have not received nearly as much interest as conventional LELSB systems it is undoubted that they offer huge benefits should their promise be realised. To achieve this; however, a recognition must be made of the additional, and different challenges which are observed in this cell format. To date the majority of research has built upon the development of solid-state electrolytes, limiting the targeted study of positive electrode architectures. Furthermore, the majority of reports have included a degree of catholyte to overcome the significant volume expansion at the positive electrode interface during operation. This is in keeping with commonly adopted practice in solid-state Li-ion cells; however clearly adds an additional interface in the cell which must be managed during operation. Given the volume expansion observed in ASSLS positive electrodes, which may be as much as an order of magnitude larger than in a Li-ion equivalent one would expect the need for catholyte to be increased. There may also be opportunities to deploy ionically conductive polymers to enhance the mechanical durability of the electrodes which may offset some of the likely requirement for catholyte in the cell. This approach has however allowed for significant benefits to be derived from the wider study of negative electrode systems in the solid-state battery field which are likely to be of great use when designing a ASSLS cell. The research must also be undertaken with a clear understanding of the minimum requirements for a practical cell which have been discussed here and elsewhere. To achieve the step-change that is required for the delivery of a full solid-state Li-S cell it is also clear that significant efforts need to be made to determine the operating mechanism of these systems. This improved mechanistic understanding would also enable the improvement of zero-excess Li systems. Finally, we believe that upon realising this insight, significant gains to the performance of the devices are likely to be achievable using finite element analysis to analyse the ionic and electronic pathways in the positive electrode and provide rational design rules for this component of the cell. Ultimately this cell format is the at the earliest technology readiness level of the Li-S cells discussed in this work, and development remains driven by research aimed at improving fundamental understanding. It is not unreasonable to expect that as the cell type matures a shift in this approach toward a more application drive design of the cell will occur, in keeping with the conventional liquid based cells discussed previously. However, there are substantial benefits to be seen by considering potential applications from the outset to accelerate developments at critical interfaces in the cell. Here, researchers will undoubtedly build upon the substantial research in the field of solid-state Li-ion technology which continues to progress at an impressive rate.

6. Conclusion & Outlook

The Li-S battery system offers compelling benefits, particularly relating to high gravimetric energy density and security and sustainability of materials supply. As a battery chemistry on the verge of widespread deployment, the potential impact of Li-S is significant; increasingly demanding, weight-sensitive applications – for example, in the electrification of flight – are likely to require systems-level gravimetric energy densities beyond what Li-ion can achieve. These markets, where weight savings are likely to attract a significant premium, will act as key early market opportunities for the Li-S system. More widely, the low-cost bill of materials and the geographically diverse materials supply provide resilient and sustainable supply chains. This deployment, however, is predicated on an ability to deliver safe systems that can deliver adequate lifetimes for given applications. In the first instance, this is likely to be significantly lower than the thousands of cycles required by the widely adopted Li-ion cell. Indeed, for cells with sufficiently high energy densities, applications exist in which ca. 100 cycles would be sufficient to allow for early market penetration.

The liquid electrolyte system has been studied for over 50 years, and there is an increasingly mature understanding of the under-pinning of reaction mechanisms; more recently, sophisticated operando tools have provided further insight into the fundamental operation of the Li-S chemistry, both revealing outstanding challenges and informing materials solutions. Historically, the liquid system has been plagued by lifetime issues, for example, associated with the polysulfide shuttle effect, and subsequent inventory loss and anode degradation. Recent strategies to mitigate this through materials optimization and reimagining of the Li-S cell mechanism are accelerating commercial deployment with clear interest being evidenced through the growth of Li-S focused companies in North America, Europe, Asia and Australia. Despite this commercial progress and improved understanding of the liquid system, it is clear that strategies to reduce or eliminate $LiNO_3$ additives, which generally have poor thermal stability, are highly beneficial. This necessity is not widely reflected in the academic literature, wherein the majority of tests still include this additive.

The recent commercial interest in Li-S cell technology has also highlighted a divergence across the sector in the cell format of

interest. Prior to the demise of Oxis Energy in 2021, the company had a dual focus on both conventional Li-S cells and quasi-solid-state cells. In more recent times, companies including Lyten and Li-S Energy appear to be primarily focusing on conventional systems, with emerging companies including Gelion, NexTech, and Molyon having publicly disclosed an interest in more solid-state type applications. More broadly, there has been disclosed interest in the use of carbonate electrolytes through Theion and sulfurized polymers as active materials by Zeta Energy. This diversity of commercial approaches highlights a degree of uncertainty as to the most viable solution to enable commercialization of the technology and the specific benefits offered by each cell format discussed in this work. It should also be noted that there is likely to be more commercial activity in this area, which will emerge, either as a material or cell developer, in the coming years, given the scale of academic interest in the literature.

As outlined in this work, there remains a significant volume of work that has attempted to move beyond the $LiNO_3$ additive. Routes to inhibit polysulfide shuttle formation and shuttle through confinement and bonding to a backbone positive electrode structure (i.e., SPAN) offer a promising route to mitigate the shuttle without deploying $LiNO_3$. However, the comparatively low sulfur loadings that are feasible using these routes require ultra-lean electrolyte loading to achieve high-energy densities in a full cell. To achieve this, it is clear that the electrolyte must be highly stable against the Li negative electrode, which has resulted in the exploration of a wide range of systems. Ultimately, the limited sulfur loadings achievable in Li-SPAN systems are likely to result in this cell being superseded in all performance metrics by alternative cell formats.

Recent progress in hybrid, non-polysulfide forming, so-called quasi-solid-state Li-S systems has disruptive potential; by suppressing the liquid phase polysulfide reactions, the shuttle effect is largely mitigated, and in turn significant lifetime extensions are possible, alongside the reduction/removal of $LiNO_3$ as a necessary component. This route also offers the potential to balance electrolyte loading against adequate sulfur loadings, as there is no need to handle the dynamic viscosity that occurs in conventional cells. As detailed in the work, this can be leveraged to manifest a cell optimized either with an optimized electrode structure for lifetime, rate and/or sulfur utilization or enable a cell to be constructed with an ultra-lean electrolyte loading enabling energy densities which are simply not feasible in the conventional liquid-electrolyte system. Importantly, these developments can be leveraged without altering the approaches that would be used to manufacture the cell. Significant developments in this area have been seen in recent years; however, the area is comparatively underexplored compared to conventional systems. Specifically, the mechanism and impact of the electrolyte choice on the mechanism of operation of the cell have not been identified with sufficient certainty. Should this be achieved, there is scope to establish critical design principles for the positive electrode. The immobilized nature of the mechanism is also likely to suit the use of advanced image-based modelling frameworks, which have been deployed to success in Li-ion systems, offering the potential for further acceleration of this technology. Given this relatively early stage in the development cycle, there are likely to be substantial improvements in lifetime, capacity, and performance through further material and electrode optimization. Additionally, there is significant scope to explore alternative electrolytes beyond the diglyme and tetraglyme systems, which are commonly used. This includes the opportunity to leverage inactive diluents to optimize the viscosity of the electrolyte and, by extension, the electrode/electrolyte interface. Finally, the electrolyte optimization for this cell may also yield positive results by focusing on reducing the specific gravity of the solvent mixture. As highlighted throughout, this work the electrolyte is by some margin the most impactful on the overall mass of a Li-S cell. By reducing the density of this crucial component whilst retaining appropriate wettability, there is scope to further optimize the energy density of the cell. These considerations should also take into account the non-active components in the electrolyte, as TTE, a reported diluent in several works, has a relatively high density of 1.54 g mL^{-1}, which provides opportunities to optimize both the composition and components of the electrolyte to target application specific performance.

In each of the systems in which a liquid electrolyte is deployed, the compatibility of the electrolyte against metallic Li remains an ongoing challenge. A commonly discussed solution to this includes the deployment of a protected Li negative electrode. Should this occur, it is likely to be informed by the significant volume of work occurring in the development of hybrid polymeric or inorganic quasi-solid state cells in which gelled electrolytes containing Li-ion conducting materials are being developed. These offer a balance between sufficient ionic conductivity and comparatively low mass to allow for practical deployment in a cell. It is important to note that, alongside the additional mass introduced to the cell, the use of a protected electrode introduces an additional interface that must be managed.

An extension of this protected electrode approach leads to fully solid-state Li-S systems. This is a nascent research field, but one with significant recent interest and promising progress in the literature. These cells face challenges associated with cathode volume change, and the risk of delaminating solid/solid interfaces, which significantly exceed those observed in the solid-state Li-ion cell and must be overcome to accelerate this field. Approaches, including the application of extreme pressures and deployment of a liquid catholyte, have been demonstrated, though these are unlikely to find use in a practical or commercial system. The use of a catholyte at the cathode/electrolyte interface has commonly been discussed to reduce the interfacial resistance and stabilize this interface in the context of Li-ion chemistries. However, in a Li-S cell, the volume changes observed are significantly larger than those observed in Li-ion cells. Alongside this, the intercalation mechanism of the Li-ion cell significantly reduces the interaction between the positive electrode and electrolyte. If catholyte is to be deployed in an ASSLSB it will need to be sufficiently inert against both the electrolyte and active material to avoid the formation of LiPS, which will result in resistance growth and capacity fade. Solving the challenges at the interface of the positive electrode and electrolyte is a critical factor that must be solved to develop this promising technology further. While this is a comparatively new field and unlikely to be deployed in the market in the near term, there are clear learnings that can be translated from the Li-ion SSB system, and from alternative Li-S cell formats, in particular the LEQSS cell format in which the positive electrode is immobilized during operation, accelerating their development. Once again, the immobilization of the positive electrode is likely to lend itself toward an ability to deploy image-based modelling

to design electrodes with particular performance characteristics. Ultimately, this cell format is the least mature, and by extension carries the greatest uncertainty over the commercialization requirements for the technology; however, it is not unrealistic to expect similar requirements, in particular on a stack pressure basis, to those discussed for the solid-state Li-ion counterpart. In this context, significant work is required to reduce the pressures applied to cells under testing from the high 10's of MPa toward a more deployable 0.5–1 MPa limit.

Ultimately, each of the cell formats discussed in this work offers routes to supersede the energy densities possible in incumbent Li-ion technologies, with their degree of maturity impacting the certainty that can be applied to this range. For conventional systems, it is feasible to consider designs that achieve in excess of 400 Wh kg^{-1}, with this having already been demonstrated in the literature. Indeed, it is likely that energy densities of approaching 500 Wh kg^{-1} are realizable with appropriate cell and component design. However, in this cell format, a coupling of the energy density and lifetime of the cell cannot be avoided due to the functional relationship between the electrolyte and the operating mechanism of the cell. This also provides a maximum practical limit on the gravimetric energy density realizable given the high mass ratio of the electrolyte in a cell, which will be between 45–60% of the total mass of the cell. Furthermore, the need to utilize $LiNO_3$ to mediate the polysulfide shuttle places significant challenges on the likelihood of passing transportation and other safety standards. Given this, the possibility of reimagining the cell in a quasi-solid-state format, in which the liquid electrolyte does not need to account for viscosity changes associated with polysulfide dissolution, offers compelling advantages to achieve high-energy cells. Most obviously, this cell format allows for the reduction of the electrolyte loading in cells from a recommended 3–5 μL $mg^{-1}{}_S$ towards values of 1.5 μL $mg^{-1}{}_S$. This low value is not achievable in a conventional system, but the reduction in electrolyte mass (in an idealized cell with equivalent parameters) provides 60% additional energy density. In practice, this additional energy density is likely to be reduced by targeting a rationally designed electrode with optimized kinetics and stability, which is likely to have a lower sulfur loading. However, this provides a compelling opportunity to realize the potential of sulfur as a positive electrode material.

The increased technology readiness level of the Li-S chemistry is demonstrated by the increased commercial focus in both start-ups and established battery manufacturers, and motivates research that focusses on clear technical challenges associated. These can be prioritized as maximizing the high energy density and lifetime of cells, and perhaps latterly their rate performance. This research, which still requires fundamental mechanistic insights and developments in material science, will, however need to be conducted with an increased focus on barriers to commercialization and deployment in the field. Of these, the continued deployment of $LiNO_3$ is perhaps the most pressing to overcome, given its embedded nature in the majority of reports in the academic literature and the significant challenge in passing existing safety standards when it is deployed in a sufficient volume to allow extended lifetime. This review highlights the breadth of activities that are ongoing to achieve this and are accelerating progress in the highly promising field of Li-S batteries towards commercial deployment.

Acknowledgements

The authors would like to acknowledge the Faraday Institution (Faraday.ac.uk; EP/S003053/1) for funding the energy storage work at the Advanced Propulsion Lab, UCL, and Department of Engineering Sciences, University of Oxford, in particular through the LiSTAR programme (FIRG083). J.B.R. would like to acknowledge Innovate UK for financial support (Project Number: 10040939). P.R.S. also acknowledged the Royal Academy of Engineering Chair in Emerging Technologies (CiET1718\59) and the Department of Science, Innovation and Technology (DSIT).

Conflict of Interest

The authors declare no conflict of interest.

Keywords

high energy density battery, lithium nitrate, lithium-sulfur battery, next generation battery chemistry, polysulfide shuttle effect

Received: June 23, 2025
Revised: September 17, 2025
Published online:

[1] J. B. Robinson, K. Xi, R. V. Kumar, A. C. Ferrari, H. Au, M.-M. Titirici, A. Parra-Puerto, A. Kucernak, S. D. S. Fitch, N. Garcia-Araez, Z. L. Brown, M. Pasta, L. Furness, A. J. Kibler, D. A. Walsh, L. R. Johnson, C. Holc, G. N. Newton, N. R. Champness, F. Markoulidis, C. Crean, R. C. T. Slade, E. I. Andritsos, Q. Cai, S. Babar, T. Zhang, C. Lekakou, N. Kulkarni, A. J. E. Rettie, R. Jervis, et al., *J.Phys.: Energy* **2021**, *3*, 031501.
[2] J. Tan, M. Ye, J. Shen, *Mater. Horizons.* **2022**, *9*, 2325.
[3] W. Li, H. Yao, K. Yan, G. Zheng, Z. Liang, Y.-M. Chiang, Y. Cui, *Nat. Commun.* **2015**, *6*, 7436.
[4] M. Zhao, B.-Q. Li, X.-Q. Zhang, J.-Q. Huang, Q. Zhang, *ACS Cent. Sci.* **2020**, *6*, 1095.
[5] J.-M. Tarascon, M. Armand, *Nature* **2001**, *414*, 359.
[6] P. G. Bruce, S. A. Freunberger, L. J. Hardwick, J.-M. Tarascon, *Nat. Mater.* **2012**, *11*, 19.
[7] S. Lang, S.-H. Yu, X. Feng, M. R. Krumov, H. D. Abruña, *Nat. Commun.* **2022**, *9*, 4811.
[8] The Faraday Institution Faraday_Insights_8_FINAL, **2020**.
[9] S. S. Zhang, *Electrochim. Acta* **2012**, *70*, 344.
[10] A. Jozwiuk, B. B. Berkes, T. Weiß, H. Sommer, J. Janek, T. Brezesinski, *Energy Environ. Sci.* **2016**, *9*, 2603.
[11] Y. Ye, M.-K. Song, Y. Xu, K. Nie, Y.-S. Liu, J. Feng, X. Sun, E. J. Cairns, Y. Zhang, J. Guo, *Energy Storage Mater.* **2019**, *16*, 498.
[12] . Recommendations on the transport of dangerous goods. Manual of tests and criteria **2015**, United Nations.
[13] S. Yari, L. Bird, S. Rahimisheikh, A. C. Reis, M. Mohammad, J. Hadermann, J. Robinson, P. R. Shearing, M. Safari, *Adv. Energy Mater.* **2024**, *14*, 2402163.
[14] A. Manthiram, S.-H. Chung, C. Zu, *Adv. Mater.* **2015**, *27*, 1980.
[15] L. Yoshida, Y. Matsui, M. Deguchi, T. Hakari, M. Watanabe, M. Ishikawa, *ACS Appl. Mater. Interf.* **2023**, *15*, 37467.
[16] L. R. Bird, J. B. Robinson, P. R. Shearing, *ACS Mater. Lett.* **2024**, *6*, 5363.
[17] G. Liu, Q. Sun, Q. Li, J. Zhang, J. Ming, *Energy Fuels* **2021**, *35*, 10405.
[18] J. Lochala, D. Liu, B. Wu, C. Robinson, J. Xiao, *ACS Appl. Mater. Interfaces* **2017**, *9*, 24407.
[19] S. Dörfler, H. Althues, P. Härtel, T. Abendroth, B. Schumm, S. Kaskel, *Joule* **2020**, *4*, p539.

[20] A. Bhargav, J. He, A. Gupta, A. Manthiram, *Joule* **2020**, *4*, 285.
[21] Y. V. Mikhaylik, J. R. Akridge, *J. Electrochem. Soc* **2004**, *151*, A1969.
[22] S. Perez-Beltran, D. Kuai, P. B. Balbuena, *ACS Energy Lett.* **2024**, *9*, 5268.
[23] Y. Luo, L. Guo, M. Xiao, S. Wang, S. Ren, D. Han, Y. Meng, *J. Mater. Chem. A* **2020**, *8*, 4629.
[24] L. C. H. Gerber, P. D. Frischmann, F. Y. Fan, S. E. Doris, X. Qu, A. M. Scheuermann, K. Persson, Y.-M. Chiang, B. A. Helms, *Nano Lett.* **2016**, *16*, 549.
[25] Y. Liao, H. Zhang, Y. Peng, Y. Hu, J. Liang, Z. Gong, Y. Wei, Y. Yang, *Adv. Energy Mater.*. **2024**, *14*, 2304295.
[26] Y.-C. Wu, S.-H. Chung, *J. Mater. Chem. A* **2023**, *14*, 9455.
[27] J. Wang, Y. Yamada, K. Sodeyama, C. H. Chiang, Y. Tateyama, A. Yamada, *Nat. Commun.* **2016**, *7*, 12032.
[28] S.-J. Tan, W.-P. Wang, Y.-F. Tian, S. Xin, Y.-G. Guo, *Adv. Funct. Mater.* **2021**, *31*, 2105253.
[29] C. Yan, H.-R. Li, X. Chen, X.-Q. Zhang, X.-B. Cheng, R. Xu, J.-Q. Huang, Q. Zhang, *J. Am. Chem. Soc.* **2019**, *141*, 9422.
[30] S. Xiong, K. Xie, Y. Diao, X. Hong, *Electrochim. Acta* **2012**, *83*, 78.
[31] R. E. Owen, W. Du, J. Millichamp, P. R. Shearing, D. J. L. Brett, J. B. Robinson, *J. Electrochem. Soc.* **2024**, *17*, 120523.
[32] S. C. Kim, X. Gao, S.-L. Liao, H. Su, Y. Chen, W. Zhang, L. C. Greenburg, J.-A. Pan, X. Zheng, Y. Ye, M. S. Kim, P. Sayavong, A. Brest, J. Qin, Z. Bao, Y. Cui, *Nat. Commun.* **2024**, *15*, 1268.
[33] Y. Liu, Y. Elias, J. Meng, D. Aurbach, R. Zou, D. Xia, Q. Pang, *Joule* **2021**, *15*, 2323.
[34] X.-Y. Li, B.-Q. Li, S. Feng, Z. Li, L. Shen, S.-Y. Sun, Z.-X. Chen, T. Jin, X. Chen, M. Zhao, X.-Q. Zhang, J.-Q. Huang, Q. Zhang, *J. Am. Chem. Soc.* **2025**, *147*, 15435.
[35] J. AKRIDGE, *Solid State Ionics* **2004**, *175*, 243.
[36] Z. W. Seh, Y. Sun, Q. Zhang, Y. Cui, *Chem. Soc. Rev.* **2016**, *45*, 5605.
[37] C. Prehal, J.-M. Sujata, S. D. Talian, A. Vizintin, R. Dominko, H. Amenitsch, L. Porcar, S. Freunberger, V. Wood, Mechanism of Li2S formation and dissolution in Lithium-Sulphur batteries, **2022** https://doi.org/10.21203/rs.3.rs-818607/v2.
[38] J.-M. von Mentlen, A. S. Güngör, T. Demuth, J. Belz, M. Plodinec, P. Dutta, A. Vizintin, L. Porcar, K. Volz, V. Wood, C. Prehal, *ACS Nano* **2025**, *19*, 16626.
[39] U. Chadha, P. Bhardwaj, S. Padmanaban, R. M. Suneel, K. Milton, N. Subair, A. Pandey, M. Khanna, D. Srivastava, R. M. Mathew, S. K. Selvaraj, M. Banavoth, P. Sonar, B. Badoni, N. S. Rao, S. G. Kumar, A. K. Ray, A. Kumar, *J. Electrochem. Soc.* **2022**, *169*, 020530.
[40] S.-H. Chung, C.-H. Chang, A. Manthiram, *Adv. Funct. Mater.* **2018**, *28*, 1801188.
[41] J. Li, L. Gao, F. Pan, C. Gong, L. Sun, H. Gao, J. Zhang, Y. Zhao, G. Wang, H. Liu, *Nano-Micro Lett.* **2024**, *16*, 12.
[42] T. Gong, X. Duan, Y. Shan, L. Huang, *Batteries* **2025**, *11*, 152.
[43] B. S. Parimalam, A. D. MacIntosh, R. Kadam, B. L. Lucht, *J. Phys. Chem. C* **2017**, *121*, 22733.
[44] S. S. Zhang, K. Xu, D. L. Foster, M. H. Ervin, T. R. Jow, *J. Power Sources* **2004**, *125*, 114.
[45] D. Aurbach, E. Pollak, R. Elazari, G. Salitra, C. S. Kelley, J. Affinito, *J. Electrochem. Soc.* **2009**, *156*, A694.
[46] M. Xu, A. Xiao, L. Yang, B. Lucht, *ECS Trans.* **2009**, *16*, 3.
[47] Y. V. Mikhaylik, US **2008**, 7354680 B2, issued Apr. 8, 2008.
[48] M. Wild, L. O'Neill, T. Zhang, R. Purkayastha, G. Minton, M. Marinescu, G. J. Offer, *Energy Environ. Sci.* **2015**, *8*, 3477.
[49] H. Yao, G. Zheng, P.-C. Hsu, D. Kong, J. J. Cha, W. Li, Z. W. Seh, M. T. McDowell, K. Yan, Z. Liang, V. K. Narasimhan, Y. Cui, *Nat. Commun.* **2014**, *5*, 3943.
[50] Z. Lin, Z. Liu, W. Fu, N. J. Dudney, C. Liang, *Adv. Funct. Mater.* **2013**, *23*, 1064.
[51] J. Wang, Z. Yao, C. W. Monroe, J. Yang, Y. Nuli, *Adv. Funct. Mater.* **2013**, *23*, 1194.
[52] R. Zhuang, S. Yao, M. Jing, X. Shen, J. Xiang, T. Li, K. Xiao, S. Qin, *Beilstein J. Nanotechnol.* **2018**, *9*, 262.
[53] S. S. Zhang, *J. Power Sources* **2016**, *322*, 99.
[54] C. Zhen, X. Yang, X. Wei, Y. Zhu, S. Han, X. Shi, L. Deng, M. D. Gu, *Nano Lett.* **2024**, *24*, 6714.
[55] F. Liu, G. Sun, H. B. Wu, G. Chen, D. Xu, R. Mo, L. Shen, X. Li, S. Ma, R. Tao, X. Li, X. Tan, B. Xu, G. Wang, B. S. Dunn, P. Sautet, Y. Lu, *Nat. Commun.* **2020**, *11*, 5215.
[56] Y. Tsao, M. Lee, E. C. Miller, G. Gao, J. Park, S. Chen, T. Katsumata, H. Tran, L.-W. Wang, M. F. Toney, Y. Cui, Z. Bao, *Joule* **2019**, *3*, 872.
[57] J. M. Cameron, C. Holc, A. J. Kibler, C. L. Peake, D. A. Walsh, G. N. Newton, L. R. Johnson, *Chem. Soc. Rev.* **2021**, *50*, 5863.
[58] J. S. Searle, F. Malagreca, B. M. G. Denison, A. J. Kibler, D. A. Walsh, L. R. Johnson, D. B. Amabilino, G. N. Newton, *ACS Energy Lett.* **2025**, *10*, 2839.
[59] B.-J. Lee, T.-H. Kang, H.-Y. Lee, J. S. Samdani, Y. Jung, C. Zhang, Z. Yu, G.-L. Xu, L. Cheng, S. Byun, Y. M. Lee, K. Amine, J.-S. Yu, *Adv. Energy Mater.* **2020**, *10*, 1903934.
[60] M. J. Zachman, Z. Tu, S. Choudhury, L. A. Archer, L. F. Kourkoutis, *Nature* **2018**, *560*, 345.
[61] S.-H. Wang, Y.-X. Yin, T.-T. Zuo, W. Dong, J.-Y. Li, J.-L. Shi, C.-H. Zhang, N.-W. Li, C.-J. Li, Y.-G. Guo, *Adv. Mater.* **2017**, *29*, 1703729.
[62] L. Zhang, M. Ling, J. Feng, L. Mai, G. Liu, J. Guo, *Energy Storage Mater.* **2018**, *11*, 24.
[63] G. Bieker, M. Winter, P. Bieker, *Phys. Chem. Chem. Phys.* **2015**, *17*, 8670.
[64] M. Sun, X. Wang, J. Wang, H. Yang, L. Wang, T. Liu, *ACS Appl. Mater. Interfaces* **2018**, *10*, 35175.
[65] C. Weller, J. Pampel, S. Dörfler, H. Althues, S. Kaskel, *Energy Technol.* **2019**, *17*, 1900625.
[66] M. Zhang, X. Zhang, S. Liu, W. Hou, Y. Lu, L. Hou, Y. Luo, Y. Liu, C. Yuan, *ChemSusChem* **2024**, *17*, 202400538.
[67] Z. Li, J. Wang, H. Yuan, Y. Yu, Y. Tan, *Adv. Funct. Mater.* **2024**, *34*, 2405890.
[68] J. Zhou, A. Sun, *Chem. Eng. J.* **2024**, *495*, 153648.
[69] X. Li, L. Yuan, D. Liu, J. Xiang, Z. Li, Y. Huang, *Small* **2022**, *18*, 2106970.
[70] S. Dörfler, S. Walus, J. Locke, A. Fotouhi, D. J. Auger, N. Shateri, T. Abendroth, P. Härtel, H. Althues, S. Kaskel, *Energy Technol.* **2021**, *9*, 2000694.
[71] S. Xin, L. Gu, N.-H. Zhao, Y.-X. Yin, L.-J. Zhou, Y.-G. Guo, L.-J. Wan, *J. Am. Chem. Soc.* **2012**, *134*, 18510.
[72] C. Kensy, D. Leistenschneider, S. Wang, H. Tanaka, S. Dörfler, K. Kaneko, S. Kaskel, *Batteries Supercaps.* **2021**, *4*, 612.
[73] Y. Xu, Y. Wen, Y. Zhu, K. Gaskell, K. A. Cychosz, B. Eichhorn, K. Xu, C. Wang, *Adv. Funct. Mater.* **2015**, *25*, 4312.
[74] H. Li, S. Ma, H. Cai, H. Zhou, Z. Huang, Z. Hou, J. Wu, W. Yang, H. Yi, C. Fu, Y. Kuang, *Energy Storage Mater.* **2019**, *18*, 338.
[75] H. Li, S. Ma, J. Li, F. Liu, H. Zhou, Z. Huang, S. Jiao, Y. Kuang, *Energy Storage Mater.* **2020**, *26*, 203.
[76] D.-W. Wang, G. Zhou, F. Li, K.-H. Wu, G. Q. M. Lu, H.-M. Cheng, I. R. Gentle, *Phys. Chem. Chem. Phys.* **2012**, *14*, 8703.
[77] L. Wang, Y. Lin, S. DeCarlo, Y. Wang, K. Leung, Y. Qi, K. Xu, C. Wang, B. W. Eichhorn, *Chem. Mater.*. **2020**, *32*, 3765.
[78] E. Markevich, G. Salitra, A. Rosenman, Y. Talyosef, F. Chesneau, D. Aurbach, *J. Mater. Chem. A* **2015**, *3*, 19873.
[79] H. M. Joseph, M. Fichtner, A. R. Munnangi, *J. Energy Chem.* **2021**, *59*, 242.
[80] X. Ji, K. T. Lee, L. F. Nazar, *Nat. Mater.* **2009**, *8*, 500.
[81] B. Zhang, X. Qin, G. R. Li, X. P. Gao, *Energy Environ. Sci.* **2010**, *3*, 1531.

[82] X. Li, J. Liang, W. Li, J. Luo, X. Li, X. Yang, Y. Hu, Q. Xiao, W. Zhang, R. Li, T.-K. Sham, X. Sun, *Chem. Mater.* **2019**, *31*, 2002.
[83] Z. Xu, J. Wang, J. Yang, X. Miao, R. Chen, J. Qian, R. Miao, *Angew. Chem., Int. Ed.* **2016**, *55*, 10372.
[84] X. Li, M. Banis, A. Lushington, X. Yang, Q. Sun, Y. Zhao, C. Liu, Q. Li, B. Wang, W. Xiao, C. Wang, M. Li, J. Liang, R. Li, Y. Hu, L. Goncharova, H. Zhang, T.-K. Sham, X. Sun, *Nat. Commun.* **2018**, *9*, 4509.
[85] M. Thommes, K. Kaneko, A. V. Neimark, J. P. Olivier, F. Rodriguez-Reinoso, J. Rouquerol, K. S. W. Sing, *Pure Appl. Chem.* **2015**, *87*, 1051.
[86] A. Senol Gungor, J.-M. von Mentlen, J. G. A. Ruthes, F. J. García-Soriano, S. Drvaric Talian, V. Presser, L. Porcar, A. Vizintin, V. Wood, C. Prehal, *ACS Appl. Mater. Interfaces* **2024**, *16*, 67651.
[87] M. Li, B. Pang, S. Dai, Y. Cui, Y. Wu, H. Li, B. Luo, *Chem. Eng. J.* **2024**, *499*, 2024.
[88] Y. Gong, J. Li, K. Yang, S. Li, M. Xu, G. Zhang, Y. Shi, Q. Cai, H. Li, Y. Zhao, *Nano-Micro Lett.* **2023**, *15*, 150.
[89] S. Niu, G. Zhou, W. Lv, H. Shi, C. Luo, Y. He, B. Li, Q.-H. Yang, F. Kang, *Carbon* **2016**, *109*, 1.
[90] M. Li, Z. Liu, Y. Zhang, X. Wang, C. Zhang, S. Zhang, *J. Solid State Electrochem.* **2021**, *25*, 1293.
[91] J. Fanous, M. Wegner, M. B. M. Spera, M. R. Buchmeiser, *J. Electrochem. Soc.* **2013**, *160*, A1169.
[92] X. Zhao, C. Wang, Z. Li, X. Hu, A. Abdul Razzaq, Z. Deng, *J. Mater. Chem. A* **2021**, *9*, 19282.
[93] X. Wang, Y. Qian, L. Wang, H. Yang, H. Li, Y. Zhao, T. Liu, *Adv. Funct. Mater.* **2019**, *29*, 1902929.
[94] J. Fanous, M. Wegner, J. Grimminger, Ä. Andresen, M. R. Buchmeiser, *Chem. Mater.* **2011**, *23*, 5024.
[95] H. Li, W. Xue, W. Xu, L. Wang, T. Liu, *Compos. Commun.*. **2021**, *24*, 100675.
[96] Y. Yao, L. Zeng, S. Hu, Y. Jiang, B. Yuan, Y. Yu, *Small.* **2017**, *13*, 1603513.
[97] R. He, Y. Li, Z. Yin, H. Liu, Y. Jin, Y. Zhang, H. Liu, X. Zhang, *ACS Appl. Energy Mater.* **2023**, *9*, 3903.
[98] G. Xie, S. Dong, A. Huo, N. Wang, *Ionics* **2022**, *23*, 2793.
[99] A. Sakuda, K. Ohara, K. Fukuda, K. Nakanishi, T. Kawaguchi, H. Arai, Y. Uchimoto, T. Ohta, E. Matsubara, Z. Ogumi, T. Okumura, H. Kobayashi, H. Kageyama, M. Shikano, H. Sakaebe, T. Takeuchi, *J. Am. Chem. Soc.* **2017**, *139*, 8796.
[100] L. Zhang, D. Liu, Z. Muhammad, F. Wan, W. Xie, Y. Wang, L. Song, Z. Niu, J. Chen, *Adv. Mater.* **2019**, *31*, 1903955.
[101] L. Jia, T. Wu, J. Lu, L. Ma, W. Zhu, X. Qiu, *ACS Appl. Mater. Interfaces* **2016**, *8*, 30248.
[102] E. D. Grayfer, E. M. Pazhetnov, M. N. Kozlova, S. B. Artemkina, V. E. Fedorov, *ChemSusChem* **2017**, *10*, 4805.
[103] H. Ye, L. Ma, Y. Zhou, L. Wang, N. Han, F. Zhao, J. Deng, T. Wu, Y. Li, J. Lu, *Proc. Natl. Acad. Sci. USA* **2017**, *114*, 13091.
[104] S. Wang, B. Lu, D. Cheng, Z. Wu, S. Feng, M. Zhang, W. Li, Q. Miao, M. Patel, J. Feng, E. Hopkins, J. Zhou, S. Parab, B. Bhamwala, B. Liaw, Y. S. Meng, P. Liu, *J. Am. Chem. Soc.* **2023**, *147*, 9624.
[105] M. Frey, R. K. Zenn, S. Warneke, K. Müller, A. Hintennach, R. E. Dinnebier, M. R. Buchmeiser, *ACS Energy Lett.*. **2017**, *2*, 595.
[106] S. Wei, L. Ma, K. E. Hendrickson, Z. Tu, L. A. Archer, *J. Am. Chem. Soc.* **2015**, *137*, 12143.
[107] Q. Pang, A. Shyamsunder, B. Narayanan, C. Y. Kwok, L. A. Curtiss, L. F. Nazar, *Nat. Energy* **2018**, *3*, 783.
[108] X. Ren, P. Gao, L. Zou, S. Jiao, X. Cao, X. Zhang, H. Jia, M. H. Engelhard, B. E. Matthews, H. Wu, H. Lee, C. Niu, C. Wang, B. W. Arey, J. Xiao, J. Liu, J.-G. Zhang, W. Xu, *Proc. Natl. Acad. Sci. USA* **2020**, *117*, 28603.
[109] J. Holoubek, H. Liu, Z. Wu, Y. Yin, X. Xing, G. Cai, S. Yu, H. Zhou, T. A. Pascal, Z. Chen, P. Liu, *Nat. Energy* **2021**, *6*, 303.
[110] X. Cao, H. Jia, W. Xu, J.-G. Zhang, *J. Electrochem. Soc.* **2021**, *168*, 010522.
[111] J. Wu, M. Li, L. Ma, X. Li, X. Chen, J. Long, Y. Wang, X. Li, J. Liu, Z. Guo, Y. Chen, *ACS Nano* **2024**, *18*, 32984.
[112] Z. Wang, B. Zhang, *Energy Materials and Devices* **2023**, *1*, 9370003.
[113] G. Cai, J. Holoubek, M. Li, H. Gao, Y. Yin, S. Yu, H. Liu, T. A. Pascal, P. Liu, Z. Chen, *Proc. Natl. Acad. Sci. USA* **2022**, *119*, 2200392119.
[114] T. Ma, Y. Ni, D. Li, Z. Zha, S. Jin, W. Zhang, L. Jia, Q. Sun, W. Xie, Z. Tao, J. Chen, *Angew. Chem., Int. Ed.* **2023**, *62*, 202310761.
[115] Y. He, P. Zou, S.-M. Bak, C. Wang, R. Zhang, L. Yao, Y. Du, E. Hu, R. Lin, H. L. Xin, *ACS Energy Lett.* **2022**, *7*, 2866.
[116] H. Asano, J. Liu, K. Ueno, K. Dokko, T. Kojima, N. Takeichi, T. Miyuki, Y. Yamakawa, M. Watanabe, *J. Power Sources* **2023**, *554*, 232323.
[117] L. Suo, Y.-S. Hu, H. Li, M. Armand, L. Chen, *Nat. Commun.* **2013**, *4*, 1481.
[118] S. Badhrinathan, H. Dai, G. P. Pandey, *Batteries Supercaps.* **2025**, *8*, 202400544.
[119] X. Ren, L. Zou, X. Cao, M. H. Engelhard, W. Liu, S. D. Burton, H. Lee, C. Niu, B. E. Matthews, Z. Zhu, C. Wang, B. W. Arey, J. Xiao, J. Liu, J.-G. Zhang, W. Xu, *Joule* **2019**, *3*, 1662.
[120] L. Yu, S. Chen, H. Lee, L. Zhang, M. H. Engelhard, Q. Li, S. Jiao, J. Liu, W. Xu, J.-G. Zhang, *ACS Energy Lett.* **2018**, *3*, 2059.
[121] S. Chen, J. Zheng, D. Mei, K. S. Han, M. H. Engelhard, W. Zhao, W. Xu, J. Liu, J.-G. Zhang, *Adv. Mater.* **2018**, *30*, 1706102.
[122] B. Pang, H. Li, Y. Guo, B. Li, F. Li, H. C, W. Parks, L. R. Bird, T. S. Miller, P. R. Shearing, R. Jervis, J. B. Robinson, *Nature* **2025**, *6*, 175.
[123] X. Ren, S. Chen, H. Lee, D. Mei, M. H. Engelhard, S. D. Burton, W. Zhao, J. Zheng, Q. Li, M. S. Ding, M. Schroeder, J. Alvarado, K. Xu, Y. S. Meng, J. Liu, J.-G. Zhang, W. Xu, *Chem* **2018**, *4*, 1877.
[124] X. Cao, L. Zou, B. E. Matthews, L. Zhang, X. He, X. Ren, M. H. Engelhard, S. D. Burton, P. Z. El-Khoury, H.-S. Lim, C. Niu, H. Lee, C. Wang, B. W. Arey, C. Wang, J. Xiao, J. Liu, W. Xu, J.-G. Zhang, *Energy Storage Mater.* **2021**, *34*, 76.
[125] Y. Liu, Y. An, C. Fang, Y. Ye, Y. An, M. He, Y. Jia, X. Hong, Y. Liu, S. Gao, Y. Hao, J. Chen, J. Zheng, Y. Lu, R. Zou, Q. Pang, *Nat. Chem.* **2025**, *17*, 614.
[126] E. Umeshbabu, B. Zheng, Y. Yang, *Electrochem.Energy Rev.* **2019**, *9*, 199.
[127] Z. Li, Z. J. Yang, J. Moloney, C. P. Yu, M. Chhowalla, *ACS Nano* **2024**, *18*, 16041.
[128] S. Das, K. N. Gupta, A. Choi, V. Pol, *Batteries* **2024**, *10*, 349.
[129] H.-D. Lim, J.-H. Park, H.-J. Shin, J. Jeong, J. T. Kim, K.-W. Nam, H.-G. Jung, K. Y. Chung, *Energy Storage Mater.* **2020**, *25*, 224.
[130] Y. Cao, P. Zuo, S. Lou, Z. Sun, Q. Li, H. Huo, Y. Ma, C. Du, Y. Gao, G. Yin, *J. Mater. Chem. A* **2019**, *7*, 6533.
[131] J. Zhou, W. Guo, C. She, Z. Zheng, K. Wang, Y. Zhu, *Appl. Mater. Today.* **2024**, *41*, 102489.
[132] R. Li, Q. Chen, J. Jian, Y. Hou, Y. Liu, J. Liu, H. Xie, J. Zhu, *J. Power Sources* **2024**, *642*, 235521.
[133] T. Shi, Y. Liao, J. Kong, H. Ji, T. Hou, Z. Huang, Y. Han, H. Xu, L. Yuan, Y. Huang, *Energy Storage Mater.* **2024**, *72*, 103744.
[134] A. Mashekova, A. Umirzakov, M. Yegamkulov, M. Aliyakbarova, B. Uzakbaiuly, A. Nurpeissova, Z. Bakenov, A. Mukanova, *RSC Advances.* **2025**, *15*, 11537.
[135] J. Gu, C. Ma, C. Dong, C. Shen, J. Ji, C. Zhou, X. Xu, L. Mai, *Small* **2024**, *20*, 2403882.
[136] W.-W. Shao, T.-K. Gao, M.-Q. Hu, Y.-T. Ni, X.-N. Fei, M.-Q. Liu, Z. Wang, L.-P. Zhou, M.-X. Jing, *J. Appl. Polym. Sci.* **2024**, *114*, 56147.
[137] D.-D. Han, S. Liu, Y.-T. Liu, Z. Zhang, G.-R. Li, X.-P. Gao, *J. Mater. Chem. A* **2018**, *6*, 18627.
[138] A. Anbunathan, K. Z. Walle, S.-H. Wu, Y.-S. Wu, J.-K. Chang, R. Jose, C.-C. Yang, *J. Energy Storage* **2024**, *93*, 112294.
[139] Z. Song, L. Wang, W. Jiang, M. Pei, B. Li, R. Mao, S. Liu, T. Zhang, X. Jian, F. Hu, *Adv. Energy Mater.*. **2024**, *14*, 2302688.

[140] X. Yu, A. Manthiram, *Adv. Funct. Mater.* **2019**, *29*, 1805996.
[141] M. Shin, A. A. Gewirth, *Adv. Energy Mater.* **2019**, *9*, 1900938.
[142] K. K. Fu, Y. Gong, B. Liu, Y. Zhu, S. Xu, Y. Yao, W. Luo, C. Wang, S. D. Lacey, J. Dai, Y. Chen, Y. Mo, E. Wachsman, L. Hu, *Sci. Adv.* **2017**, *3*.
[143] Q. Wang, J. Guo, T. Wu, J. Jin, J. Yang, Z. Wen, *Solid State Ionics* **2017**, *300*, 67.
[144] T.-T. Zuo, Y. Shi, X.-W. Wu, P.-F. Wang, S.-H. Wang, Y.-X. Yin, W.-P. Wang, Q. Ma, X.-X. Zeng, H. Ye, R. Wen, Y.-G. Guo, *ACS Appl. Mater. Interf.*. **2018**, *10*, 30065.
[145] X. Judez, H. Zhang, C. Li, G. G. Eshetu, Y. Zhang, J. A. González-Marcos, M. Armand, L. M. Rodriguez-Martinez, *J. Phys. Chem. Lett.* **2017**, *18*, 3473.
[146] G. G. Eshetu, X. Judez, C. Li, O. Bondarchuk, L. M. Rodriguez-Martinez, H. Zhang, M. Armand, *Angew. Chem., Int. Ed.* **2017**, *56*, 15368.
[147] X. Judez, G. G. Eshetu, I. Gracia, P. López-Aranguren, J. A. González-Marcos, M. Armand, L. M. Rodriguez-Martinez, H. Zhang, C. Li, *ChemElectroChem* **2019**, *6*, 326.
[148] J. T. Kim, H. Su, Y. Zhong, C. Wang, H. Wu, D. Zhao, C. Wang, X. Sun, Y. Li, *Nat. Chem. Eng.* **2024**, *1*, 400.
[149] C. Monroe, J. Newman, *J. Electrochem. Soc.* **2004**, *151*, A880.
[150] X. Zhang, Q. Xiang, S. Tang, A. Wang, X. Liu, J. Luo, *Nano Lett.* **2020**, *4*, 2871.
[151] B. Qi, X. Hong, Y. Jiang, J. Shi, M. Zhang, W. Yan, C. Lai, *Nano-Micro Lett.* **2024**, *16*, 71.
[152] F. Zhang, Y. Guo, L. Zhang, P. Jia, X. Liu, P. Qiu, H. Zhang, J. Huang, *eTransportation* **2023**, *15*, 100220.
[153] J.-M. Doux, Y. Yang, D. H. S. Tan, H. Nguyen, E. A. Wu, X. Wang, A. Banerjee, Y. S. Meng, *J. Mater. Chem. A* **2020**, *8*, 5049.
[154] Z. Lin, Z. Liu, W. Fu, N. J. Dudney, C. Liang, *Angew. Chem., Int. Ed.* **2013**, *52*, 7460.
[155] T. Hakari, A. Hayashi, M. Tatsumisago, *Adv. Sustain. Syst.* **2017**, *1*, 1700017.
[156] C. Cui, Q. Ye, C. Zeng, S. Wang, X. Xu, T. Zhai, H. Li, *Energy Storage Mater.* **2022**, *45*, 814.
[157] H. Zhang, C. Li, M. Piszcz, E. Coya, T. Rojo, L. M. Rodriguez-Martinez, M. Armand, Z. Zhou, *Chem. Soc. Rev.* **2017**, *46*, 797.
[158] F. Liu, J. Wang, W. Chen, M. Yuan, Q. Wang, R. Ke, G. Zhang, J. Chang, C. Wang, Y. Deng, J. Wang, M. Shao, *Adv. Mater.* **2024**, *36*, 2409838.
[159] R. Chen, Q. Li, X. Yu, L. Chen, H. Li, *Chem. Rev.* **2020**, *14*, 6820.
[160] J. B. Robinson, K. Xi, R. V. Kumar, A. C. Ferrari, H. Au, M.-M. Titirici, A. Parra-Puerto, A. Kucernak, S. D. S. Fitch, N. Garcia-Araez, Z. L. Brown, M. Pasta, L. Furness, A. J. Kibler, D. A. Walsh, L. R. Johnson, C. Holc, G. N. Newton, N. R. Champness, F. Markoulidis, C. Crean, R. C. T. Slade, E. I. Andritsos, Q. Cai, S. Babar, T. Zhang, C. Lekakou, N. Kulkarni, A. J. E. Rettie, R. Jervis, et al., *J. Phys. Energy.* **2021**, *3*, 031501 .
[161] M. Pasta, D. Armstrong, Z. L. Brown, J. Bu, M. R. Castell, P. Chen, A. Cocks, S. A. Corr, E. J. Cussen, E. Darnbrough, V. Deshpande, C. Doerrer, M. S. Dyer, H. El-Shinawi, N. Fleck, P. Grant, G. L. Gregory, C. Grovenor, L. J. Hardwick, J. T. S. Irvine, H. J. Lee, G. Li, E. Liberti, I. McClelland, C. Monroe, P. D. Nellist, P. R. Shearing, E. Shoko, W. Song, D. S. Jolly, et al., *J. Phys.: Energy* **2020**, *2*, 032008.
[162] J. Janek, W. G. Zeier, *Nat. Energy* **2023**, *8*, 230.
[163] J. Sung, J. Heo, D.-H. Kim, S. Jo, Y.-C. Ha, D. Kim, S. Ahn, J.-W. Park, *Mater. Chem. Front.* **2024**, *8*, 1861.
[164] S. Bandyopadhyay, B. Nandan, *Mater. Today Energy.* **2023**, *31*, 101201.
[165] A. Deshmukh, M. Thripuranthaka, V. Chaturvedi, A. K. Das, V. Shelke, M. V. Shelke, *Progress Energy.* **2022**, *4*, 042001.
[166] X. Gao, X. Zheng, Y. Tsao, P. Zhang, X. Xiao, Y. Ye, J. Li, Y. Yang, R. Xu, Z. Bao, Y. Cui, *J. Am. Chem. Soc.* **2021**, *143*, 18188.
[167] J. T. Kim, X. Hao, C. Wang, X. Sun, *Matter* **2023**, *6*, 316.
[168] D. Cao, X. Sun, F. Li, S.-M. Bak, T. Ji, M. Geiwitz, K. S. Burch, Y. Du, G. Yang, H. Zhu, *Angew. Chem., Int. Ed.* **2023**, *62*, 202302363.
[169] J. T. Kim, A. Rao, H.-Y. Nie, Y. Hu, W. Li, F. Zhao, S. Deng, X. Hao, J. Fu, J. Luo, H. Duan, C. Wang, C. V. Singh, X. Sun, *Nat. Commun.* **2023**, *14*, 6404.
[170] L. Wang, T. Zhang, S. Yang, F. Cheng, J. Liang, J. Chen, *J. Energy Chem.* **2013**, *22*, 72.
[171] Y.-C. Lu, Q. He, H. A. Gasteiger, *J. Phys. Chem. C* **2014**, *118*, 5733.
[172] Z. Yang, Z. Zhu, J. Ma, D. Xiao, X. Kui, Y. Yao, R. Yu, X. Wei, L. Gu, Y.-S. Hu, H. Li, X. Zhang, *Adv. Energy Mater.* **2016**, *6*, 1600806.
[173] S. Randau, D. A. Weber, O. Kötz, R. Koerver, P. Braun, A. Weber, E. Ivers-Tiffée, T. Adermann, J. Kulisch, W. G. Zeier, F. H. Richter, J. Janek, *Nat. Energy* **2020**, *5*, 259.
[174] C. Ye, S. Xu, H. Li, J. Shan, S.-Z. Qiao, *Adv. Mater.* **2024**, *37*, 2407738.
[175] F. Liang, S. Wang, Q. Liang, A. Zhong, C. Yang, J. Qian, H. Song, R. Chen, *Adv. Energy Mater.*. **2024**, *14*, 2401959.
[176] K. B. Hatzell, *Joule* **2020**, *4*, 719.
[177] H. Liu, Y. Chen, P.-H. Chien, G. Amouzandeh, D. Hou, E. Truong, I. P. Oyekunle, J. Bhagu, S. W. Holder, H. Xiong, P. L. Gor'kov, J. T. Rosenberg, S. C. Grant, Y.-Y. Hu, *Nat. Mater.* **2025**, *25*, 581.
[178] Z. Ning, D. S. Jolly, G. Li, R. De Meyere, S. D. Pu, Y. Chen, J. Kasemchainan, J. Ihli, C. Gong, B. Liu, D. L. R. Melvin, A. Bonnin, O. Magdysyuk, P. Adamson, G. O. Hartley, C. W. Monroe, T. J. Marrow, P. G. Bruce, *Nat. Mater.* **2021**, *20*, 1121.
[179] S. Narayanan, U. Ulissi, J. S. Gibson, Y. A. Chart, R. S. Weatherup, M. Pasta, *Nat. Commun.* **2022**, *13*, 7237.
[180] S. Ohno, W. G. Zeier, *Acc. Mater. Res.*. **2021**, *2*, 869.
[181] X. Yang, J. Luo, X. Sun, *Chem. Soc. Rev.* **2020**, *49*, 2140.
[182] J. Wu, J. Li, X. Yao, *Adv. Funct. Mater.* **2025**, *39*, 2416671.
[183] Y. Pilyugina, E. V. Kuzmina, V. S. Kolosnitsyn, *ECS J. Solid State Sci. Technol.* **2024**, *13*, 065011.
[184] S. Li, L. Li, H. Yang, Y. Zhao, Y. Shan, *Chem. Eng. J.* **2024**, *484*, 149433.
[185] P. Jiang, G. Du, J. Cao, X. Zhang, C. Zou, Y. Liu, X. Lu, *Energy Technol.* **2023**, *11*, 2201288.
[186] X. Judez, H. Zhang, C. Li, J. A. González-Marcos, Z. Zhou, M. Armand, L. M. Rodriguez-Martinez, *J. Phys. Chem. Lett.* **2017**, *8*, 1956.
[187] G. G. Eshetu, X. Judez, C. Li, M. Martinez-Ibañez, I. Gracia, O. Bondarchuk, J. Carrasco, L. M. Rodriguez-Martinez, H. Zhang, M. Armand, *J. Am. Chem. Soc.* **2018**, *140*, 9921.
[188] Z. Ao, Y. Zou, H. Zou, Y. Huang, N. Chen, *Chem. – A Eur. J.* **2022**, *28*, 202200543.
[189] H.-M. Wang, M. Geng, J. Bai, D. Zhou, W. Hua, S. Liu, X. Gao, *Mater. Horizons.* **2025**, *12*, 141.
[190] J. Lee, C. Zhao, C. Wang, A. Chen, X. Sun, K. Amine, G.-L. Xu, *Chem. Soc. Rev.* **2024**, *53*, 5264.
[191] D. Y. Oh, Y. J. Nam, K. H. Park, S. H. Jung, S-J. Cho, Y. K. Kim, Y.-G. Lee, S.-Y. Lee, Y. S. Jung, *Adv. Energy Mater.* **2015**, *5*, 1500865.
[192] J. Li, J. Fleetwood, W. B. Hawley, W. Kays, *Chem. Rev.* **2022**, *112*, 903.
[193] R. Tao, Y. Gu, Z. Du, X. Lyu, J. Li, *Nature Rev. Clean Technol.* **2025**, *1*, 116.
[194] S. Kim, Y. A. Chart, S. Narayanan, M. Pasta, *Nano Lett.* **2022**, *22*, 10176.
[195] I. Kochetkov, T.-T. Zuo, R. Ruess, B. Singh, L. Zhou, K. Kaup, J. Janek, L. Nazar, *Energy Environ. Sci.* **2022**, *15*, 3933.
[196] H. Kwak, J.-S. Kim, D. Han, J. S. Kim, J. Park, G. Kwon, S.-M. Bak, U. Heo, C. Park, H.-W. Lee, K.-W. Nam, D.-H. Seo, Y. S. Jung, *Nat. Commun.* **2023**, *14*, 2459.
[197] T. Asano, A. Sakai, S. Ouchi, M. Sakaida, A. Miyazaki, S. Hasegawa, *Adv. Mater.* **2018**, *30*, 1803075.
[198] Q. Wang, Y. Zhou, X. Wang, H. Guo, S. Gong, Z. Yao, F. Wu, J. Wang, S. Ganapathy, X. Bai, B. Li, C. Zhao, J. Janek, M. Wagemaker, *Nat. Commun.* **2024**, *15*, 1050.

[199] Y. Wang, T. Liu, L. Estevez, J. Kumar, *Energy Storage Mater.* **2020**, *27*, 232.
[200] A. Hayashi, T. Ohtomo, F. Mizuno, K. Tadanaga, M. Tatsumisago, *Electrochem. Commun.*. **2003**, *5*, 701.
[201] M. Agostini, Y. Aihara, T. Yamada, B. Scrosati, J. Hassoun, *Solid State Ionics* **2013**, *244*, 48.
[202] S. Ohno, R. Koerver, G. Dewald, C. Rosenbach, P. Titscher, D. Steckermeier, A. Kwade, J. Janek, W. G. Zeier, *Chem. Mater.* **2019**, *31*, 2930.
[203] M. Chen, S. Adams, *J. Solid State Electrochem.* **2015**, *19*, 697.
[204] Q. Zhang, N. Huang, Z. Huang, L. Cai, J. Wu, X. Yao, *J. Energy Chem.* **2020**, *40*, 151.
[205] M. Pavan, K. Münch, S. L. Benz, T. Bernges, A. Henss, W. G. Zeier, J. Janek, *Chem. Mater.* **2025**, *37*, 3185.
[206] J. P. Mwizerwa, Q. Zhang, F. Han, H. Wan, L. Cai, C. Wang, X. Yao, *ACS Appl. Mater. Interfaces* **2020**, *12*, 18519.
[207] T. Inada, T. Kobayashi, N. Sonoyama, A. Yamada, S. Kondo, M. Nagao, R. Kanno, *J. Power Sources* **2009**, *194*, 1085.
[208] D. Wang, L.-J. Jhang, R. Kou, M. Liao, S. Zheng, H. Jiang, P. Shi, G.-X. Li, K. Meng, D. Wang, *Nat. Commun.* **2023**, *14*, 1895.
[209] P. Chen, H. Qu, D. Zheng, X. Zhang, D. Qu, *Adv. Funct. Mater.* **2025**, *35*, 2423633.
[210] H. Nagata, Y. Chikusa, J. Akimoto, *J. Power Sources* **2020**, *453*, 227905.
[211] H. Song, K. Münch, X. Liu, K. Shen, R. Zhang, T. Weintraut, Y. Yusim, D. Jiang, X. Hong, J. Meng, Y. Liu, M. He, Y. Li, P. Henkel, T. Brezesinski, J. Janek, Q. Pang, *Nature* **2025**, *637*, 846.
[212] C. Tan, T. M. M. Heenan, R. F. Ziesche, S. R. Daemi, J. Hack, M. Maier, S. Marathe, C. Rau, D. J. L. Brett, P. R. Shearing, *ACS Appl. Energy Mater.* **2018**, *1*, 5090.
[213] A. Yermukhambetova, C. Tan, S. R. Daemi, Z. Bakenov, J. A. Darr, D. J. L. Brett, P. R. Shearing, *Sci. Rep.* **2016**, *6*, 35291.
[214] C. Tan, M. D. R. Kok, S. R. Daemi, D. J. L. Brett, P. R. Shearing, *Phys. Chem. Chem. Phys.* **2019**, *21*, 4145.
[215] C. Heubner, S. Maletti, H. Auer, J. Hüttl, K. Voigt, O. Lohrberg, K. Nikolowski, M. Partsch, A. Michaelis, *Adv. Funct. Mater.* **2021**, *31*, 2106608.
[216] K. Yoon, S. Lee, K. Oh, K. Kang, *Adv. Mater.* **2022**, *34*, 2104666.
[217] S. Y. Kim, J. Li, *Energy Mater. Adv.* **2021**, *2021*.
[218] T. Wang, J. Duan, B. Zhang, W. Luo, X. Ji, H. Xu, Y. Huang, L. Huang, Z. Song, J. Wen, C. Wang, Y. Huang, J. B. Goodenough, *Energy Environ. Sci.* **2022**, *15*, 1325.
[219] Y.-G. Lee, S. Fujiki, C. Jung, N. Suzuki, N. Yashiro, R. Omoda, D.-S. Ko, T. Shiratsuchi, T. Sugimoto, S. Ryu, J. H. Ku, T. Watanabe, Y. Park, Y. Aihara, D. Im, I. T. Han, *Nat. Energy* **2020**, *5*, 299.
[220] D. Spencer-Jolly, V. Agarwal, C. Doerrer, B. Hu, S. Zhang, D. L. R. Melvin, H. Gao, X. Gao, P. Adamson, O. V. Magdysyuk, P. S. Grant, R. A. House, P. G. Bruce, *Joule* **2023**, *7*, 503.
[221] J. A. Lewis, K. A. Cavallaro, Y. Liu, M. T. McDowell, *Joule* **2022**, *6*, 1418.
[222] J. Yu, X. Sun, X. Shen, D. Zhang, Z. Xie, N. Guo, Y. Wang, *Energy Storage Mater.* **2025**, *76*, 104134.
[223] J. Zhang, J. Fu, P. Lu, G. Hu, S. Xia, S. Zhang, Z. Wang, Z. Zhou, W. Yan, W. Xia, C. Wang, X. Sun, *Adv. Mater.*. **2025**, *37*, 2413499.
[224] M. Burton, S. Narayanan, B. Jagger, L. F. Olbrich, S. Dhir, M. Shibata, M. J. Lain, R. Astbury, N. Butcher, M. Copley, T. Kotaka, Y. Aihara, M. Pasta, *Nat. Energy* **2024**, *10*, 135.
[225] I. Ellerington, High-energy battery technologies **2020**, *Faraday Report*, https://faraday.ac.uk/wp-content/uploads/2020/01/High-Energy-battery-technologies-FINAL.pdf.
[226] S. Nanda, A. Gupta, A. Manthiram, *Adv. Energy Mater.*. **2018**, *8*, 1801556.
[227] H. Ye, M. Li, T. Liu, Y. Li, J. Lu, *ACS Energy Lett.*. **2020**, *5*, 2234.
[228] Y. Yang, G. Zheng, S. Misra, J. Nelson, M. F. Toney, Y. Cui, *J. Am. Chem. Soc.* **2012**, *134*, 15387.
[229] J. H. Cruddos, J. B. Robinson, P. R. Shearing, A. J. E. Rettie, *J. Phys.: Energy* **2025**, *7*, 025006.
[230] J. He, A. Bhargav, A. Manthiram, *ACS Energy Lett.* **2022**, *7*, 583.
[231] Y. Zhao, L. Huang, D. Zhao, J. Yang Lee, *Angew. Chem., Int. Ed.* **2023**, *62*, 202308976.
[232] B. Jin, T. Lai, A. Manthiram, *ACS Energy Lett.* **2023**, *8*, 3767.
[233] X. Meng, Y. Liu, L. Yu, J. Qiu, Z. Wang, *Adv. Funct. Mater.* **2023**, *33*, 2211062.
[234] H. Cheng, C. Gao, N. Cai, M. Wang, *Chem. Commun.* **2021**, *57*, 3708.
[235] Y. Zhao, H. Ye, H. Zhang, D. Zhao, L. Huang, J. Y. Lee, *Mater. Today Energy.* **2022**, *30*, 101179.

Yiheng Shao is a PhD researcher at the Department of Engineering Science, University of Oxford. He is affiliated with the ZERO institute at the University of Oxford and the LiSTAR research program at The Faraday Institution. He obtained his MEng degree in Chemical Engineering with honours from Imperial College London in 2024. His research currently focuses on the 4D visualisation of lithiumsulfur battery degradation.

Boyi Pang is a PhD candidate at the Advanced Propulsion Laboratory (APL) at University College London. He earned his MSc in Advanced Materials Science from UCL with distinction, having previously completed his undergraduate studies at Harbin Institute of Technology in China. His research focuses on realizing the quasi-solid-state conversion process of sulfur to enhance the rate performance and cycle life of lithium-sulfur batteries, while investigating the conversion mechanisms of sulfur. His research interests also extend to next-generation lithium-ion and sodium-ion batteries, as well as advanced carbon materials.

Liam Bird received their MEng in Energy Engineering from the University of East Anglia in 2017. They completed their PhD in Graphene Technology from the University of Cambridge in 2024, with a focus on developing operando Raman mapping techniques for lithium-sulfur cells. They are currently a Faraday Institution research fellow on the LiSTAR project at the University of Oxford, and their research focus is the characterisation and analysis of lithium-sulfur cathodes using X-ray computed tomography.

James Robinson is an Associate Professor of Advanced Propulsion at University College London. He is the Co-Principal Investigator of the Faraday Institution funded LiSTAR programme which is aiming to advance lithium sulfur battery technology. Alongside this he is particularly interested in electrochemical energy storage for aerospace applications and the development of diagnostic and characterisation techniques for battery technologies.

Paul Shearing is a Professor of Sustainable Energy Engineering at the Department of Engineering Science and Director of the ZERO Institute at Oxford University. He holds the Royal Academy of Engineering Chair in Emerging Battery Technologies. His research interests center on the characterization and understanding of materials for batteries and other energy applications with a major focus on the development of new X-ray techniques. He was a founding investigator of The Faraday Institution, the UK's independent institute for electrochemical energy storage research where he leads the LiSTAR and Safebatt research programs.